Available online at www.sciencedirect.com
SCIENCE DIRECT®
Journal of Chromatography A, 1037 (2004) 191–221
JOURNAL OF CHROMATOGRAPHY A
www.elsevier.com/locate/chroma

Review

Determination of isotherms by gas–solid chromatography Applications

Fani Roubani–Kalantzopoulou*

School of Chemical Engineering, National Technical University of Athens, 9 Iroon Polytechniou St., 15780 Zografou, Athens, Greece

Abstract

This literature review of the fundamental developments in gas–solid adsorption isotherms includes articles published from 1933 until now. Analytical and numerical methods used for calculating the adsorption energy distribution function, as a quantitative measure of surface heterogeneity, are included. Special attention is paid to inverse gas chromatography (IGC) and more precisely to a new version of IGC known as reversed-flow gas chromatography (RF-IGC or RF-GC). RF-GC is presented as a quick, precise and effective method to investigate physicochemical properties of different kinds of adsorbents, through adsorption isotherms and related energetic parameter determinations. Advantages of the RF-GC method over traditional chromatographic methods are discussed.

Keywords: Reviews; Adsorption isotherms; Gas–solid chromatography; Reversed-flow gas chromatography; Inverse gas chromatography; Time resolved chromatography; Probability density function; Adsorption; Mathematical modelling

Contents

* Tel.: +30-210-7723-277; fax: +30-210-2027-691.
E-mail address: roubanif@central.ntua.gr (F. Roubani–Kalantzopoulou).

0021-9673/$ – see front matter © 2004 Elsevier B.V. All rights reserved.
doi:10.1016/j.chroma.2003.12.005

1. Fundamentals of adsorption

Thermodynamics of surfaces had been studied by Butler [1] and Guggenheim [2], but no clear thermodynamic treatment of the physical adsorption of gases by solids was made until the 1940s. In the next two decades the work of Hill [3,4] and Everett [5] is the most important, while more recently Rusanov [6], Jovanovic [7], Everett [8], Steele [9], Rudzinski and Sokolowski [10] have contributed in this investigation. Steele and Rudzinski among others have studied the effects of intermolecular forces at low surface coverage.

A potential function $U(x, y, z)$ can describe the interaction energy of an isolated adsorbed molecule with the adsorbent, where x, y, z are the Cartesian coordinates of the adsorbed molecule. The form of this $U(x, y, z)$ function characterize a surface. Fig. 1, that it is from Ref. [11], shows all the cases with a theoretical or practical interest. Thus, $U(x, y, z)$ is constant for a homogeneous surface (cf. Fig. 1a), while in the case of a heterogeneous surface a series of minima and maxima (cf. Fig. 1d–f), are appeared. The differences between the energy of the minima and the average energy of molecules in the equilibrium is (are) the "energy (ies) of site (es) adsorption". This energy is denoted by ΔU^0. In the case of a constant value of the local minima U_m the surface is "a homogeneous site surface"(cf. Fig. 1c). If the oscillations in U are much less than kT, the surface may be described as "a homogeneous periodic surface"(cf. Fig. 1b). In the case where oscillations in U greatly exceed kT the local U_m are the "adsorption sites or adsorption centres". If a periodicity exists which is characterized by minima with different values of U_m the surface may be called "a heterogeneous periodic surface"(cf. Fig. 1d). In many real surfaces with defects of various kinds distributed at random the surface is "a random heterogeneous surface", since the potential function $U(x, y, z)$ is no longer periodic (cf. Fig. 1e). Moreover, "a patch-wise heterogeneous surface" (cf. Fig. 1f). is appeared in the case of different crystal faces, each of which is a homogeneous site surface. The energy barrier between sites, which controls lateral diffusion, is called the activation energy for the surface diffusion ΔV^0.

A high adsorption energy corresponds to a large negative value of ΔU, since the adsorption energies are conventionally given a positive sign.

On the other hand, experimental adsorption isotherms $\Theta(T, p)$ represents an average over all values of the adsorption energies existing on the gas–solid interface, while the function $\theta(\varepsilon, T, p)$ is traditionally called "local adsorption isotherm".

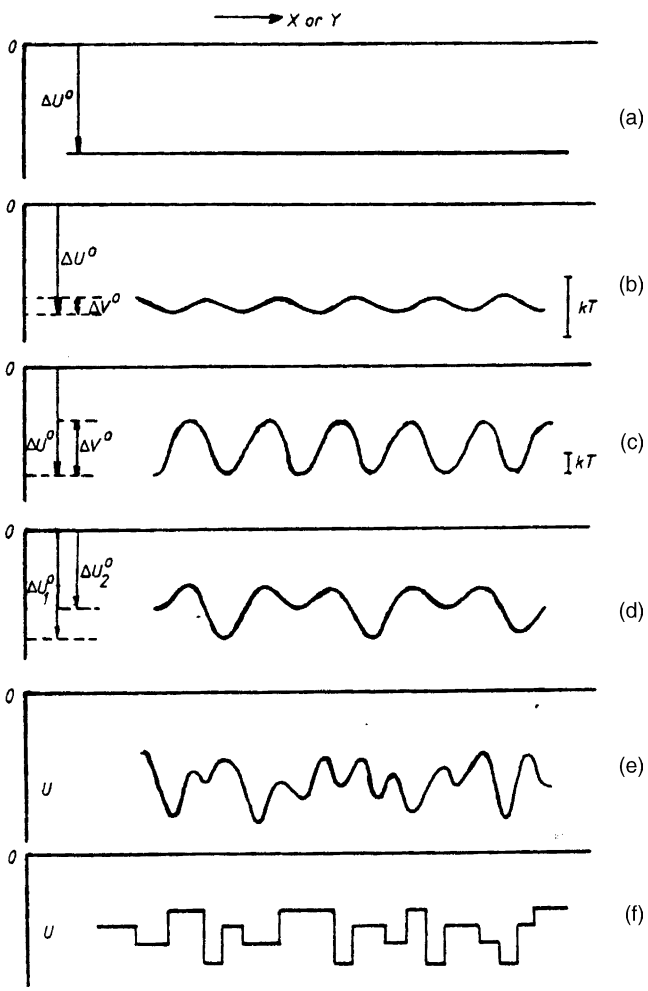

Fig. 1. (a) Perfectly homogeneous surface; (b) homogeneous periodic surface; (c) homogeneous site surface; (d) heterogeneous periodic surface; (e) random heterogeneous surface; (f) patch-wise heterogeneous surface corresponding to (a). From Ref. [11] with permission.

The adsorption sites exhibiting various values of adsorption energies are distributed over the solid surface. This distribution is called "topography of the surface". This dispersion of adsorption energy is the so-called surface heterogeneity [11]. Its measure is the distribution of adsorption energy or probability density function for the adsorption energies. The studies of the effect of adsorption energy dispersion on the behavior of adsorption system have constituted one of the most dynamic world trends in the research on adsorption for the last few decades.

There are some scientific efforts for the study of adsorption on homogeneous surfaces based on localized and

mobile adsorption. There are two comprehensive works in the literature with detailed reviews concerning the theories of localized adsorption written by Domb [12] and Clark [13].

As regards the mobile adsorption the first treatment was Devonshire's theory [14]. A great number of new theories have appeared from 1970 til now. The basic assumption of the theoretical models is that the molecules interact via a potential, which is a function of the intermolecular distance, taking into account the repulsive interactions. The Van der Waals model simplifies the solution under certain conditions. Finally, the related isotherm equation is found.

2. Topography of surfaces

Three models of topography of surfaces were considered in the studies of adsorption on heterogeneous surfaces. Thus, when the adsorption energy distribution, that is the way in which the adsorption centres of various energies are distributed on the solid surface, as well as the interactions between the adsorbing molecules, are taken into account three types can be seen:

(a) the patch-wise type (cf. Fig. 2A);
(b) the random (cf. Fig. 2B); and
(c) the intermediate (cf. Fig. 2C).

The patch-wise type was for the first time used by Ross and Olivier [15]. In this the adsorption centres of the same properties are grouped in patches. These patches are so large that they constitute independent thermodynamic adsorption parameters. For instance, in the case of crystals with a few crystallographic planes this model is the most suitable.

The random model was used by Hill [16]. This model assumes that the adsorption sites of various adsorption energies are distributed on the surface in a random way. Amorphous samples are representative examples of solid compounds where this random model is justified. These are two boundary cases. The surfaces are commonly characterized by the intermediate surface topography [17].

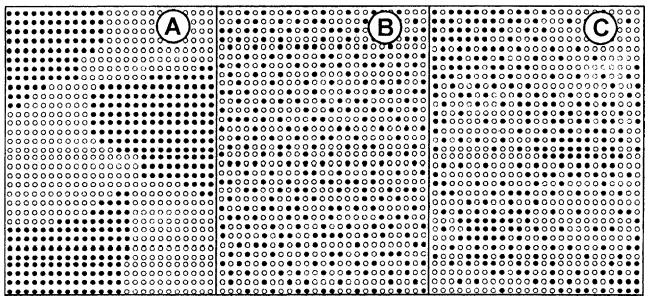

Fig. 2. Diagram concerning the topography of the surface of the adsorbent. (A) The patch-wise type; (B) the random type and (C) the intermediate type. From Ref. [17] with permission.

3. Adsorption integral isotherms

One of the main objectives of much of the earlier work was to examine the possibility of providing a theoretical basis for some of the empirical equations by assuming that the surface heterogeneity could be characterized by a particular mathematical form of the distribution of adsorption energies among adsorption sites. The inverse process of deducing information on the nature of surface heterogeneity, i.e. of retrieving the adsorption energy distribution, from measured adsorption isotherms was initiated by Drain and Morrisson and co-workers [18–22], Adamson and Ling [23], and Ross and co-workers [22,24,25]. This aspect is still a very active area of research.

There is a large and growing literature on the numerical solution of integral equations, among which are several monographs [26–28]. One reason for the sheer volume of activity is that there are many different kinds of equations, each with many different algorithms have been proposed to deal with a single case. Although, while composing a new algorithm, authors usually have taken into consideration the shortcomings of the previous ones, an ultimate procedure for the solution of the linear Fredholm integral equation of the first kind, Eq. (1), has not been elaborated yet.

$$\int K(x, y) f(y)\, \mathrm{d}y = g(x) \tag{1}$$

Thus, new efforts are needed to improve the methods of analysis of this problem. First, the new proposed method should be faster than those previously proposed and should enable one to attain approximately the same accuracy. Second, that formulation of a minimization problem should exclude an unphysical value of unknown and evaluated function (i.e. strong oscillations, a negative value of a probabilistic distribution function, and so on). Moreover, the program code of the algorithm should be simple, short, and easy for application for the wide group of scientists [26].

The analysis of physical adsorption data has become a standard method of assessment of the energetic and structural heterogeneity of solid adsorbents [26,29–36]. The theoretical description of adsorption on heterogeneous solids is usually interpreted by the superposition of adsorption on independent homogeneous sorption sites and/or in pores with the same widths. In the past 25 years considerable progress in the analysis of these quantities has been achieved due to the appearance of advanced numerical methods for solving the unstable linear Fredholm integral equation of the first kind.

A universal procedure for the characterization of solid adsorbents connected with choosing numerical methods for the evaluation of structural and geometric heterogeneity does not exist. A comprehensive review of different methods of the solution of the integral equation (the condensation approximation, regularization methods and non-negative least-squares methods) can be found for example, in three basic monographs [11,35,36]. On the other hand, estimating

the distribution function from Eq. (1) is a well-known ill-posed (incorrect) problem, which is manifested by the fact that there exists an infinitely large set of possible solutions, all satisfying Eq. (1) with the accuracy of the experimental error. In other words, all solutions may have arbitrary large deviations from each other (and from the true solution) but they can fit the experimental data well at the same time.

To select a meaningful solution of the unstable linear Fredholm integral equation of the first kind from a set of all possible solutions, a number of the most famous and successful algorithms have been described by different authors:

(a) Heterogeneity investigated at loughborough by distribution analysis (HILDA), the Jaycock and House method [37].
(b) Adamson–Ling distribution analysis (ALINDA) [23,38,39].
(c) Computed adsorption energy distribution in the monolayer (CAEDMON), the Ross and Morrison method [22,40].
(d) Computed adsorption energies using singular value decompositions analysis result (CAESAR) [38,41].
(e) Energy distribution computation from adsorption isotherms utilizing the smoothing spline functions (EDCAIS) [42].
(f) REMEDI is essentially similar to the regularization method proposed by House [43].
(g) Solution of adsorption integral equation using splines (SAIEUS) [44].
(h) Solution of adsorption integral equation (INTEG) [45].
(i) Improved regularization algorithm (IRA) [46].
(j) Expectation maximization (EM) [47].
(k) CONTIN [48–50].
(l) REG [51].
(m) Methods based on Stieltjes and Laplace transforms (MEBSLT) [11].
(n) Methods based on Fourier transform (MEBFT) [11,52].
(o) Rudzinski–Jagiello method (MEBRJ) [11,53].

It is very interesting that the majority of the above mentioned methods have been proposed for the evaluation of the energy distribution functions. The INTEG algorithm and the CONTIN package are two methods also being successfully used for the estimation of the pore size distribution of adsorbents. The main assumptions of the last methods are described in Ref. [26]. Further investigations have been made recently through some new works [54–57] and a Polish–Japanese cooperation [58–61].

4. Determination of adsorption isotherms and related energetic parameters using nonlinear inverse chromatography

Non-linear non-ideal gas–solid chromatography offers a unique means of studying thermodynamics parameters of adsorption and adsorption isotherms at very low surface coverage, a region of concentrations very important in characterizing the structure of the solid surface. Such physicochemical measurements have been described in detail in three books [62–64].

Dynamic measurements by means of gas adsorption chromatography have become a very popular and powerful method of investigating adsorption phenomena. Kiselev and Yashin [62] have shown that in a case of heterogeneous surfaces (where the elution peak is strongly asymmetrical), the pressure dependence of the net retention volume can be measured easily.

Adsorption isotherms by gas chromatography until 1976 were mostly determined by using frontal analysis (FA), frontal analysis by characteristic point (FACP) and elution by characteristic point (ECP). Details can be found in two monographs [63,64]. Later, the step and pulse method combined the frontal analysis and the elution method. It carries out conventional gas chromatographic measurements of retention times, using as carrier gas a mixture of an inert gas and the vapor of the compound under study. The vapor concentration is constant during an experiment and adjusted between measurements to scan the desired range. This constant concentration measurement is the *step*. Very small *pulses* of vapor or perturbation are injected, and their retention times are observed. The relation of the retention time of the pulses with the isotherm sought has been derived in detail [65,66]. The method does not give directly an independent experimental isotherm. However, a significant advantage of determining the adsorption isotherm by a chromatographic method is its sensitivity to the slope of the adsorption isotherm and thus the ability of the chromatographic method to determine the slope with a constant precision over the whole range of the surface coverage. This is important in modelling the adsorption behavior.

On the other hand, adsorption energy distribution of solute probes on heterogeneous surfaces has been determined from their nonlinear chromatographic band profiles for the last 30 years by Inverse Chromatography. The general problem of obtaining distribution functions from adsorption isotherms data has proceeded for a substantially longer period of time. The basic fundamental hurdle is centered around the solution of the linear Fredholm integral of the first kind:

$$Q(p) = \int_{\min \varepsilon}^{\varepsilon \max} \theta(\varepsilon p) f(\varepsilon)\, \mathrm{d}\varepsilon \tag{2}$$

where $Q(p)$ is the experimentally measured global adsorption isotherm as a function of the solute partial pressure, p; $\theta(\varepsilon p)$ is the local model of adsorption for each adsorption site of energy, ε; and $f(\varepsilon)$ is the distribution function of interest. In order to accelerate research in this area chromatographic retention volumes may be used to obtain the adsorption isotherm. Stanley and Guiochon have dealt with the estimation of adsorption energy distribution from nonlinear chromatographic data [67] from theoretical and experimental point of view. The experimental data was obtained on silica

samples. While the theoretical models of adsorption studied were the Langmuir, Jovanovic, Fowler–Guggenheim (both random and patch-wise) and Brunnauer–Emmett–Teller local isotherms.

In another work [68] Guiochon proposed a new Jovanovic–Freundlich isotherm model for describing single-component adsorption equilibria on heterogeneous surfaces. The equation reduces to the Jovanovic equation when the surface becomes homogeneous. At low pressures, the equation reduces to the Freundlich isotherm but at high pressures, a monolayer coverage is achieved. The fit of the experimental data to the new model described is shown to be better than the comparable fits to classical isotherms used for heterogeneous surfaces. The energy distribution function corresponding to the model for Langmuir local adsorption behavior was based on the Sips procedure.

Rubio et al. have studied the energy distribution functions corresponding to the adsorption of several molecular probes on four sodium silicoborates. These have been obtained from their adsorption isotherms through a frontal analysis [69].

Bakaev et al. used the inverse gas chromatography for the study of the heterogeneity of E-glass fibers through adsorption measurements [70].

Some other chromatographic methods relating to adsorption isotherms may be found in the literature [71–78].

Recently, a new chromatographic perturbation method is used by Kalogirou et al. [79] for studying adsorption–desorption equilibrium in various gas/solid heterogeneous systems. It is the reversed-flow one giving accurate and precise values of many physicochemical constants, among which the basic and necessary adsorption isotherm values are included. For four inorganic oxides, namely, Cr_2O_3, Fe_2O_3, TiO_2 and PbO, and two aromatic hydrocarbons, (benzene, toluene) these adsorption isotherms have been determined through a non-linear model.

5. Experimental adsorption isotherms in gas–solid systems determined by reversed-flow gas chromatography

Progress in many areas of material science and engineering requires the development of new advanced methods for studying processes taking place at phase-boundaries. That is the case of the reversed-flow gas chromatographic (RF-GC) technique, which is a tool for studying gas–solid interfaces [80–84]. Ref. [81] is an interesting book by Katsanos (the pioneer of this chromatographic method) describing the RF-GC method in detail. From this point of view the RF-GC method differs from the classical chromatographic methods, being interested in the stationary phase properties rather than the solute ones. Thus, it provides information about the material surface nature and behavior in various environments, including individual material properties and air pollution influence on them. From another point of view, traditional inverse gas–solid chromatography [85] has about the same aims, but as it is a classical chromatographic elution method, it has several weak points.

It does not take into account the sorption effect, it neglects the mass-transfer phenomena taking place, and also it is influenced by the carrier gas flow.

The RF-GC method takes into account all the above and even more, the desorption stage, which is often neglected. Thus, with the use of suitable personal computer programs, [84,86] the study of the absorption/desorption phenomena of many gases on many solids become possible by the RF-GC method without specifying a priori an adsorption isotherm equation. Two significant advantages of this method are simplicity and low cost in relation to the time required.

The physicochemical study in [79] is a case study, which focuses on the experimental examination of some powders that are used in the processing of paint and ceramic industry as well as in catalyst preparation and utilization. In contrast to the work accomplished with the same RF-GC method based on a linear model [87], this study is based on a non-linear-adsorption isotherm model [83,86], which is the appropriate for studying oxides and generally materials other than metals. The failure of a linear model in this case is attributed to surface heterogeneity of these substances [88].

As adsorption of mixture of gases and vapors on solids is of significant interest in many diverse areas of Chemistry various forms of perturbation chromatography have been used to measure pure-component isotherms and in few cases even binary isotherms. A systematic study of two binary systems: C_6H_6–NO_2 and $C_6H_5CH_3$–NO_2 on five adsorbents including ZnO, Cr_2O_3, TiO_2, PbO, Fe_2O_3, is presented by Roubani-Kalantzopoulou [89]. Determination of these binary isotherms on well-characterized adsorbents will provide the data base needed for the development of the models to analyze and interpret such data. In an analogous publication [90] RF-GC has been used to measure physicochemical constants among which binary isotherms and adsorption–desorption as well as reaction rate constants of 21 heterogeneous systems including TiO_2 (or PbO or Fe_2O_3), as a solid and a binary gas system. The last one is comprised of NO_2 and an aliphatic or aromatic hydrocarbon: C_2H_6, C_2H_4, C_2H_2, C_3H_6, 1-C_4H_8,C_6H_6,$C_6H_5CH_3$. The precision and accuracy of the method are discussed.

Similarly, RF-GC was used to study the kinetics of the action of five hydrocarbons namely, ethane, ethene, ethyne, propene and butene and of the nitrogen dioxide, on three known and widely used pigments, the white one TiO_2, and the yellows CdS and $PbCrO_4$ [91]. The calculation of kinetic parameters and mass transfer coefficients is based on an experimental adsorption isotherm. All these calculations are based on a non linear adsorption isotherm model as it is well accepted that the linear one is inadequate for inorganic substances like these mentioned in this work. The inadequacy is mainly attributed to the non-uniformity of the solid surface. Five physicochemical parameters have been obtained for each of the twenty heterogeneous reactions

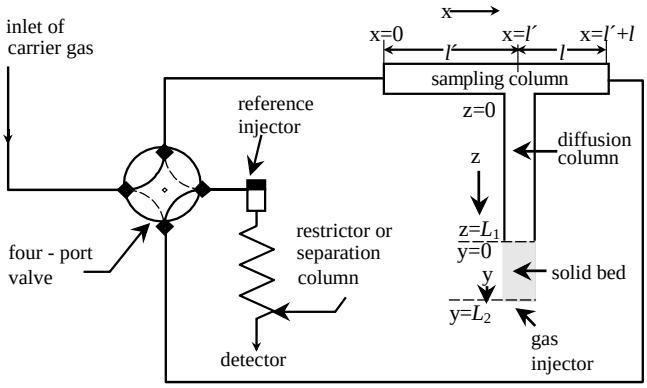

Fig. 3. The experimental set-up of RF-GC for studying adsorption isotherms. From Refs. [109,110] with permission.

studied. Some of the calculations were based on the linear model for comparison.

In parallel, in [92] a physicochemical study of the influence of ethene and ethyne on various Greek marbles is presented, in terms of adsorption isotherms and kinetic constants. All these works as well as some others as [93–95] have been done with the same experimental set-up (cf. Fig. 3), while in some previous works, which have been summarized in a review [96] the RF-GC technique was used in connection with diffusion denuder tubes (cf. Fig. 4).

Thus, a contribution to environmental catalysis is done by RF-GC, through measurements, mechanism and models [89–96].

With the same methodology another scientific group have published interesting results concerning diffusion and catalysis [97–107]. More precisely, the adsorption of gases on Pt–Rh bimetallic catalysts, as well as the kinetics for the oxidation of carbon monoxide in the presence of excess of oxygen over Pt–Rh alloy catalysts was studied among others using the RF-GC.

RF-GC is extended recently to the measurements of the probability density function for the adsorption energies as well as the differential energies of adsorption due to lateral interactions of molecules adsorbed on different heterogeneous solid surfaces. All these calculations are based on a non-linear adsorption isotherm model as it is well accepted that the linear one is inadequate for substances with heterogeneous surface. Thus, some new important physicochemical parameters have been obtained experimentally for the characterization of the heterogeneous systems studied. As a case study here the adsorption of many significant hydrocarbons was investigated. With these systematic experiments under conditions similar to the atmospheric ones, an extrapolation of the results obtained to "real" atmospheres with a high degree of confidence is possible. Many recent publications may be found in the literature concerning these objectives [108–113], while Refs. [114,115] are two previous reviews concerning models, mechanisms and applications of the RF-GC method.

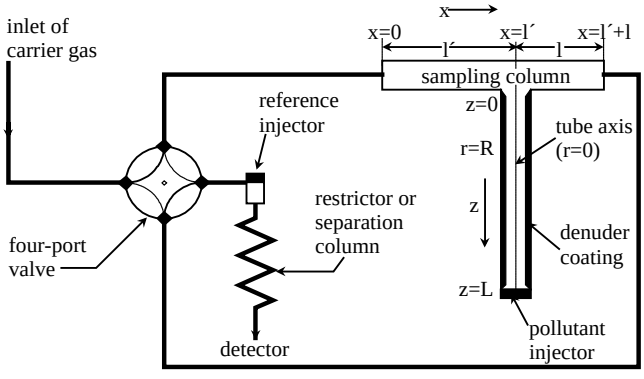

Fig. 4. Experimental set-up of RF-IGC combined with a denuder tube for environmental studies. From Ref. [84] with permission.

6. The reversed-flow gas chromatography method

6.1. Theoretical analysis of adsorption isotherms determination

The theoretical analysis dealing with physicochemical parameters determination under non-steady-state conditions, has been published elsewhere [94,114,115]. Only the absolutely necessary mathematical equations are quoted here to help the reader understand how the parameters in Tables 1–10 and Figs. 6–16 published in this review were extracted from the experimental data.

First, the local adsorption isotherm of the gas adsorbate studied:

$$c_S^* = \frac{m_S}{a_S} \cdot \delta(y - L_2) + \frac{a_y}{a_S} \cdot k_1 \int_0^t c_y(\tau)\, d\tau \quad (3)$$

where c_S^* is the equilibrium adsorbed concentration of the gas adsorbate at time t (mol g^{-1}), m_S the initially adsorbed amount of this gas adsorbate (mol), a_S the amount of solid material per unit length of column bed (g cm^{-1}), $\delta(y - L_2)$ the Dirac's delta function for the initial condition of the bed, when the gas adsorbate is introduced as an instantaneous pulse at the point $y = L_2$ (cm^{-1}), y the length coordinate along section L_2 (cm), a_y the cross-sectional area of the void space in region y (cm^2), k_1 the local adsorption parameter (s^{-1}), c_y the gaseous concentration of the adsorbate as a function of time t and coordinate y along the column (mol cm^{-3}) and τ the dummy variable for time.

Second, the mass balance equation for the gas adsorbate in the gaseous region z of the diffusion column:

$$\frac{\partial c_z}{\partial t} = D_1 \cdot \frac{\partial^2 c_z}{\partial z^2} - k_{app} c_z. \quad (4)$$

where c_z is the gaseous concentration of the gas adsorbate as a function of time t and length coordinate z along the column (mol cm^{-3}), D_1 the diffusion coefficient of this gas adsorbate into the carrier gas (cm^2 s^{-1}) and k_{app} the apparent

Table 1
Sample isotherms for the adsorption of benzene and toluene on PbO at 363.2 and 393.2 K, respectively

Dummy variable (min)	Benzene on PbO			Toluene on PbO		
	$(\partial c_S^* \partial c_G)$ ($cm^3\,g^{-1}$)	c_S^* ($mol\,g^{-1}$)	c_G ($mol\,cm^{-3}$)	$(\partial c_S^* \partial c_G)$ ($cm^3\,g^{-1}$)	c_S^* ($mol\,g^{-1}$)	c_G ($mol\,cm^{-3}$)
20	0.9176	1.034×10^{-8}	2.229×10^{-8}	−0.5548	6.957×10^{-9}	2.983×10^{-8}
25	0.3086	9.543×10^{-9}	2.046×10^{-8}	0.3660	6.218×10^{-9}	2.932×10^{-8}
30	0.2359	8.830×10^{-9}	1.775×10^{-8}	0.1899	5.525×10^{-9}	2.648×10^{-8}
35	0.2159	8.220×10^{-9}	1.503×10^{-8}	0.1484	4.914×10^{-9}	2.279×10^{-8}
40	0.2151	7.707×10^{-9}	1.263×10^{-8}	0.1322	4.397×10^{-9}	1.907×10^{-8}
45	0.2261	7.274×10^{-9}	1.066×10^{-8}	0.1257	3.967×10^{-9}	1.573×10^{-8}
50	0.2474	6.907×10^{-9}	9.111×10^{-9}	0.1248	3.614×10^{-9}	1.290×10^{-8}
55	0.2792	6.591×10^{-9}	7.904×10^{-9}	0.1278	3.324×10^{-9}	1.060×10^{-8}
60	0.3225	6.315×10^{-9}	6.980×10^{-9}	0.1344	3.085×10^{-9}	8.778×10^{-9}
65	0.3781	6.069×10^{-9}	6.273×10^{-9}	0.1448	2.886×10^{-9}	7.349×10^{-9}
70	0.4463	5.846×10^{-9}	5.729×10^{-9}	0.1594	2.719×10^{-9}	6.243×10^{-9}

From Ref. [79] with permission.

rate constant of a first-order or pseudofirst-order reaction of the gas adsorbate in the gas phase (s^{-1}).

Next, the mass balance equation of the same gas adsorbate in region y of the diffusion column, filled with the solid material under study:

$$\frac{\partial c_y}{\partial t} = D_2 \cdot \frac{\partial^2 c_y}{\partial y^2} - k_{-1}\frac{a_S}{a_y}(c_S^* - c_S) - k_{app}c_y \quad (5)$$

where D_2 is the diffusion coefficient of this gas adsorbate into the gas phase in section y ($cm^2\,s^{-1}$), k_{-1} the rate constant for desorption of the solute from the solid bulk (s^{-1}) and c_S the concentration of the gas adsorbate adsorbed on the solid at time t ($mol\,g^{-1}$).

Table 2
Sample isotherms at 323.2 K for the adsorption of 2 cm^3 ethene on Penteli marble,where $\partial c_S^*/\partial c_R$ (cm^3/g^{-1}) is the differential isotherm, c_S^* (mol/g^{-1}) is the integrated isotherm and c_R (mol/cm^{-3}) is the gaseous concentration at r=R, of Fig. 4

Reversal time t (min)	$\partial c_S^*/\partial c_R$ ($cm^3\,g^{-1}$)	∂c_S^* ($\times 10^{-7}\,mol\,g^{-1}$)	c_R ($\times 10^{-8}\,mol\,cm^{-3}$)
5	3.9213	8.7489	9.8201
10	6.5105	7.3758	7.0595
15	9.0767	6.3239	5.7004
20	10.5784	5.4522	4.8182
25	11.1889	4.7086	4.1376
30	11.3866	4.0681	3.5711
35	11.4347	3.5149	3.0865
40	11.4349	3.0366	2.6684
45	11.4222	2.6232	2.3066
50	11.4077	2.2659	1.9936
55	11.3946	1.9570	1.7227
60	11.3836	1.6902	1.4884
65	11.3746	1.4596	1.2858
70	11.3673	1.2605	1.1107
75	11.3614	1.0885	0.9593
80	11.3566	0.9399	0.8285
85	11.3528	0.8116	0.7155
90	11.3497	0.7008	0.6179
95	11.3472	0.6051	0.5336
100	11.3452	0.5225	

From Ref. [92] with permission.

Finally, the rate of change of the adsorbed concentration:

$$\frac{\partial c_S}{\partial t} = k_{-1}(c_S^* - c_S) - k_2 c_S \quad (6)$$

where k_2 is the rate constant of a possible first-order or pseudofirst-order surface reaction of the adsorbed solute (s^{-1}).

With the initial conditions $c_y(0, y) = (m/a_y)\cdot\delta(y - L_2)$, and $c_S(0, y) = 0$, m being the amount (mol) of the gas adsorbate introduced as a pulse at $y = L_2$, the solution of the system of differential Eqs. (3)–(6) leads to the function:

$$H^{1/M} = gc(l', t) = \sum_{i=1}^{4} A_i \exp(B_i t) \quad (7)$$

where H is the height of sample peaks resulting from the flow reversal (cm), M the response factor of the detector

Table 3
The dependence of deposition velocities (V_d) and reaction probabilities (γ) on the gaseous pollutant, the marble and the working temperature

Gas–solid system	T (K)	V_d ($\times 10^{-7}\,ms^{-1}$)	$10^9\gamma$
C_2H_2–$CaCO_3$	313.2	3.0 ± 0.8	2.4 ± 0.7
C_2H_2–$CaCO_3$	323.2	3.50 ± 0.20	2.73 ± 0.15
C_2H_2–$CaCO_3$	333.2	5.9 ± 1.9	4.5 ± 1.5
C_2H_2–Karistos marble	313.2	2.2 ± 0.7	1.7 ± 0.6
C_2H_2–Karistos marble	323.2	3.6 ± 0.7	2.8 ± 0.5
C_2H_2–Karistos marble	333.2	5.7 ± 1.9	4.4 ± 1.5
C_2H_2–Kavala marble	313.2	4.0 ± 1.6	3.2 ± 1.3
C_2H_2–Kavala marble	333.2	7.0 ± 3.0	5.9 ± 2.3
C_2H_2–Penteli marble	313.2	5.0 ± 2.3	4.0 ± 1.8
C_2H_2–Penteli marble	323.2	6.8 ± 2.5	5.3 ± 1.4
C_2H_4–Karistos marble	313.2	2.3 ± 0.5	1.9 ± 0.4
C_2H_4–Karistos marble	323.2	6.0 ± 0.6	4.9 ± 0.5
C_2H_4–Karistos marble	333.2	17.3 ± 6.2	13.08 ± 0.13
C_2H_4–Kavala marble	313.2	4.1 ± 2.3	3.4 ± 0.9
C_2H_4–Kavala marble	323.2	5.5 ± 0.5	4.4 ± 0.9
C_2H_4–Penteli marble		2.6 ± 1.0	2.1 ± 0.9

From Ref. [92] with permission.

Table 4
The differential isotherms for the adsorption of five aliphatic hydrocarbons on PbO at 323.2 K

Dummy variable (min)	C_2H_6–NO_2–PbO		C_2H_4–NO_2–PbO		C_2H_2–NO_2–PbO		C_3H_6–NO_2–PbO		1-C_4H_8–NO_2–PbO	
	$(\partial c_S^*/\partial c_G)$ ($cm^3\,g^{-1}$)	c_G ($mol\,cm^{-3}$)	$(\partial c_S^*/\partial c_G)$ ($cm^3\,g^{-1}$)	c_G ($mol\,cm^{-3}$)	$(\partial c_S^*/\partial c_G)$ ($cm^3\,g^{-1}$)	c_G ($mol\,cm^{-3}$)	$(\partial c_S^*/\partial c_G)$ ($cm^3\,g^{-1}$)	c_G ($mol\,cm^{-3}$)	$(\partial c_S^*/\partial c_G)$ ($cm^3\,g^{-1}$)	c_G ($mol\,cm^{-3}$)
15	6.298	2.493×10^{-8}	6.921×10^{-2}	2.637×10^{-8}	0.6736	3.033×10^{-8}	−0.3597	1.947×10^{-8}	−2.171	1.779×10^{-8}
20	2.268	2.383×10^{-8}	5.246×10^{-2}	2.438×10^{-8}	0.4761	2.779×10^{-8}	0.4083	1.942×10^{-8}	1.918	1.767×10^{-8}
25	1.769	2.216×10^{-8}	4.870×10^{-2}	2.227×10^{-8}	0.4236	2.496×10^{-8}	0.2205	1.860×10^{-8}	1.102	1.686×10^{-8}
30	1.609	2.036×10^{-8}	4.753×10^{-2}	2.025×10^{-8}	0.4044	2.223×10^{-8}	0.1847	1.753×10^{-8}	0.9422	1.582×10^{-8}
35	1.546	1.861×10^{-8}	4.715×10^{-2}	1.839×10^{-8}	0.3974	1.973×10^{-8}	0.1726	1.641×10^{-8}	0.8960	1.476×10^{-8}
40	1.521	1.696×10^{-8}	4.702×10^{-2}	1.670×10^{-8}	0.3957	1.750×10^{-8}	0.1677	1.531×10^{-8}	0.8874	1.374×10^{-8}
45	1.512	1.545×10^{-8}	4.699×10^{-2}	1.515×10^{-8}	0.3964	1.551×10^{-8}	0.1656	1.426×10^{-8}	0.8947	1.279×10^{-8}
50	1.511	1.406×10^{-8}	4.698×10^{-2}	1.375×10^{-8}	0.3982	1.375×10^{-8}	0.1647	1.328×10^{-8}	0.9094	1.192×10^{-8}
55	1.512	1.280×10^{-8}	4.699×10^{-2}	1.248×10^{-8}	0.4005	1.220×10^{-8}	0.1642	1.236×10^{-8}	0.9277	1.112×10^{-8}
60	1.514	1.166×10^{-8}	4.701×10^{-2}	1.133×10^{-8}	0.4030	1.084×10^{-8}	0.1638	1.151×10^{-8}	0.9476	1.039×10^{-8}
65	1.517	1.062×10^{-8}	4.703×10^{-2}	1.028×10^{-8}	0.4055	9.632×10^{-9}	0.1635	1.071×10^{-8}	0.9680	9.727×10^{-9}
70	1.519	9.671×10^{-9}	4.705×10^{-2}	9.336×10^{-9}	0.4080	8.566×10^{-9}	0.1632	9.963×10^{-9}	0.9883	9.115×10^{-9}
75	1.521	8.809×10^{-9}	4.707×10^{-2}	8.475×10^{-9}	0.4103	7.623×10^{-9}	0.1628	9.268×10^{-9}	1.008	8.553×10^{-9}
80	1.523	8.026×10^{-9}	4.710×10^{-2}	7.694×10^{-9}	0.4126	6.788×10^{-9}	0.1623	8.620×10^{-9}	1.027	8.035×10^{-9}
85	1.525	7.313×10^{-9}	4.712×10^{-2}	6.985×10^{-9}	0.4147	6.049×10^{-9}	0.1617	8.016×10^{-9}	1.044	7.556×10^{-9}
90	1.527	6.664×10^{-9}	4.715×10^{-2}	6.341×10^{-9}	0.4167	5.393×10^{-9}	0.1610	7.452×10^{-9}	1.061	7.113×10^{-9}
95	1.528	6.034×10^{-9}	4.718×10^{-2}	5.758×10^{-9}	0.4186	4.811×10^{-9}	0.1600	6.925×10^{-9}	1.076	6.702×10^{-9}

From Ref. [90] with permission.

Table 5
Simple and binary adsorption isotherms for three oxides. The influence of NO_2 is apparent

Gases	Fe_2O_3		PbO		TiO_2	
	Minimum $c_s^* \times 10^{-9}$	Maximum $c_s^* \times 10^{-9}$	Minimum $c_s^* \times 10^{-9}$	Maximum $c_s^* \times 10^{-9}$	Minimum $c_s^* \times 10^{-9}$	Maximum $c_s^* \times 10^{-9}$
C_2H_6	19.86	98.89	2.70	11.98	0.10	0.51
C_2H_6–NO_2	4.23	22.05	8.48	44.39	9.18	45.27
C_2H_4	0.02	0.13	26.63	157.30	1558.92	8539.29
C_2H_4–NO_2	6.55	40.74	0.28	1.40	109.31	643.65
C_2H_2	17.35	116.45	918.55	6665.51	8.37	54.39
C_2H_2–NO_2	10.38	72.41	2.06	14.33	2707.20	17818.23
C_3H_6	0.02	0.07	2.23	7.77	242439.70	793575.20
C_3H_6–NO_2	0.61	2.11	1.17	3.82	43716.16	147538.50
1-C_4H_8	9.23	24.30	2.88	6.34	18.31	41.32
1-C_4H_8–NO_2	487.73	1236.85	7.73	20.75	45.53	107.50

From Ref. [90] with permission.

Table 6
Dynamic adsorption rate constants (k_1), desorption rate constants (k_{-1}), surface reaction rate constants (k_2), of five aliphatic hydrocarbons interacting with TiO_2 in the presence of NO_2 at 323.2 K. The goodness of curve fitting is given by the squared correlation coefficient for both the four exponential and the three exponential functions (r_4^2, r_3^2)

Heterogeneous System	k_1 (s^{-1})	k_{-1} (s^{-1})	k_2 (s^{-1})	r_4^2	r_3^2
C_2H_6–NO_2–TiO_2	1.30×10^{-3}	5.49×10^{-3}	8.11×10^{-5}	0.9994	0.9994
C_2H_4–NO_2–TiO_2	3.86×10^{-2}	1.36×10^{-3}	3.47×10^{-4}	0.9994	0.9994
C_2H_2–NO_2–TiO_2	7.31×10^{-1}	2.19×10^{-6}	1.41×10^{-4}	0.9995	0.9995
C_3H_6–NO_2–TiO_2	1.43	6.30×10^{-7}	1.46×10^{-3}	0.9986	0.9976
1-C_4H_8–NO_2–TiO_2	3.13×10^{-4}	1.33×10^{-2}	1.97×10^{-3}	0.9979	0.9974

From Refs. [90,91] with permission.

(dimensionless), g the calibration factor of the detector ($cm\,mol^{-1}\,cm^3$) and $c(l', t)$ the sampling concentration of the gas adsorbate measured ($mol\,cm^{-3}$).

The explicit calculation of the isotherm can be carried out as described elsewhere [83]. However, the following equations are improved [114], as they are based on Eq. (7), rather than on Eq. (8), as was done originally [83].

$$H^{1/M} = gc(l', t) = \sum_{i=1}^{3} A_i \exp(B_i t) \tag{8}$$

$$\frac{\partial c_S^*}{\partial c_G} = k_1 \cdot \frac{a_y \sum_{i=1}^{4} A_i \exp(B_i \tau)}{a_s \sum_{i=1}^{4} A_i B_i \exp(B_i \tau)} \tag{9}$$

$$c_S^* = \frac{k_1 a_y}{g a_S} \cdot \sum_{i=1}^{4} A_i \exp(B_i \tau)/B_i \tag{10}$$

$$c_G = \frac{1}{g} \cdot \sum_{i=1}^{4} A_i \exp(B_i \tau) \tag{11}$$

where c_G is the gaseous concentration of the probe gas ($mol\,cm^{-3}$), and A_i and B_i are the pre-exponential factors and the exponential coefficients of Eq. (7). One can consider τ in the above equations as a dummy independent variable and calculate, for chosen arbitrary values of τ, both the differential isotherm $\partial c_S^*/\partial c_G$ and c_S^*, together with the corresponding values of c_G. Plotting $\partial c_S^*/\partial c_G$ or c_S^* against c_G for

Table 7
Dynamic adsorption rate constants (k_1), desorption rate constants (k_{-1}), surface reaction rate constants (k_2), of C_6H_6 or $C_6H_5CH_3$ ($3.2 \times 10^{-3}\,mol\,dm^{-3}$), interacting with the surface of three oxides at 363.2 and 393.2 K, respectively. The goodness of curve fitting is given by the squared correlation coefficient for both the four exponential and the three exponential functions (r_4^2, r_3^2)

Heterogeneous system	k_1 (s^{-1})	k_{-1} (s^{-1})	k_2 (s^{-1})	r_4^2	r_3^2
C_6H_6–NO_2–Fe_2O_3	6.81×10^{-4}	1.30×10^{-2}	7.15×10^{-4}	0.9974	0.9910
$C_6H_5CH_3$–NO_2–Fe_2O_3	439×10^{-4}	4.65×10^{-3}	1.07×10^{-3}	0.9994	0.9620
C_6H_6–NO_2–PbO	4.28×10^{-4}	5.72×10^{-2}	1.31×10^{-3}	0.9990	0.9989
$C_6H_5CH_3$–NO_2–PbO	2.82×10^{-4}	9.87×10^{-4}	3.64×10^{-3}	0.9996	0.9889
C_6H_6–NO_2–TiO_2	7.99×10^{-4}	4.33×10^{-3}	1.00×10^{-3}	0.9985	0.9423
$C_6H_5CH_3$–NO_2–TiO_2	9.03×10^{-4}	2.16×10^{-3}	1.19×10^{-3}	0.9926	0.8890

From Refs. [90,93] with permission.

Table 8
Mean values for the systems: C_2H_6–NO_2–TiO_2, C_2H_4–NO_2–TiO_2, C_2H_2–NO_2–TiO_2

C_2H_6–NO_2–TiO_2	$\ln A_1$	10.94 ± 0.04
	B_1	−0.0190 ± 0.0003
	$\ln A_2$	7.2 ± 0.4
	B_2	−0.029 ± 0.005
	$\ln A_3$	11.219 ± 0.019
	B_3	−0.1730 ± 0.0025
C_2H_4–NO_2–TiO_2	$\ln A_1$	11.057 ± 0.008
	B_1	−0.02108 ± 0.00008
	$\ln A_2$	10.8 ± 0.5
	B_2	−0.157 ± 0.019
	$\ln A_3$	10.35 ± 0.09
	B_3	−0.249 ± 0.013
C_2H_2–NO_2–TiO_2	$\ln A_1$	11.354 ± 0.015
	B_1	−0.02150 ± 0.00014
	$\ln A_2$	10.7 ± 0.5
	B_2	−0.072 ± 0.012
	$\ln A_3$	12.00 ± 0.13
	B_3	−0.157 ± 0.007

From Ref. [90] with permission.

each chosen τ, independent experimental isotherms are obtained.

6.2. Theoretical analysis of energetic physicochemical quantities

The RF-GC method does not depend on analytical or numerical solutions of the classical integral Eq. (12) [36], but on a time function of the extra chromatographic peaks (cf. Fig. 5) obtained by short flow-reversals of the carrier gas, as Eq. (13) shows [86,92,114,115].

$$\Theta(p, T) = \int_0^\infty \theta_i(p, T, \varepsilon)\, f(\varepsilon)\, \mathrm{d}\varepsilon \tag{12}$$

$$H^{1/M} = \sum_{i=1}^{4} A_i \exp(B_i t) \tag{13}$$

where $\Theta(p,T)$ is the overall experimental adsorption isotherm, $\theta(p,T,\varepsilon)$ the local isotherm, $f(\varepsilon)$ the probability density function for the adsorption energies, H is the peak height, M the response factor of the detector, A_i the pre-exponential factors, and B_i the exponential coefficients of time t, when flow reversals are made.

The main equation of the experimental technique as well as of the corresponding model is Eq. (13). The calculation of A_i and B_i values from the experimental points H, t, and their physical content have been reported many times [86,114,115]. The relevant mathematical model was based on the following four equations:

The mass balance equation for the analyte in the gaseous region z of the diffusion column:

$$\frac{\partial c_z}{\partial t} = D_1 \cdot \frac{\partial^2 c_z}{\partial z^2} - k_{\mathrm{app}} c_z \tag{14}$$

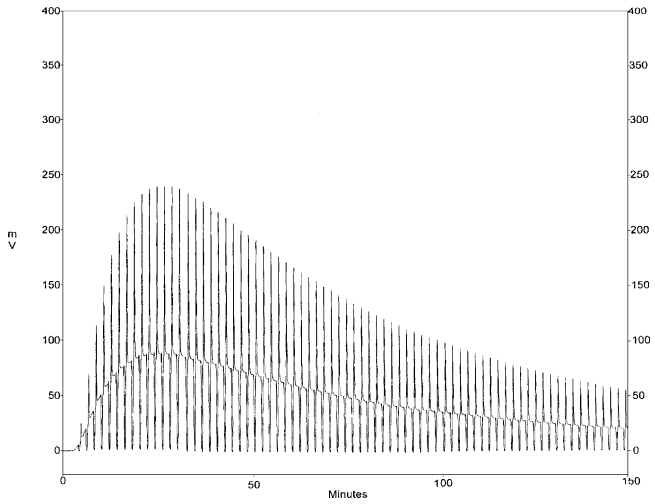

Fig. 5. Sample peaks obtained by RF-GC. From Ref. [125] with permission.

The mass balance equation for the same analyte in the region y of the diffusion column, filled with the solid material under study:

$$\frac{\partial c_y}{\partial t} = D_2 \cdot \frac{\partial^2 c_y}{\partial y^2} - k_{-1} \cdot \frac{a_{\mathrm{S}}}{a_y}(c_{\mathrm{S}}^* - c_{\mathrm{S}}) - k_{\mathrm{app}} c_y \tag{15}$$

The rate of change of the adsorbed concentration on the heterogeneous solid surface:

$$\frac{\partial c_{\mathrm{S}}^*}{\partial t} = k_{-1}(c_{\mathrm{S}}^* - c_{\mathrm{S}}) - k_2 c_{\mathrm{S}} \tag{16}$$

The local adsorption isotherm of the analyte is:

$$c_{\mathrm{S}}^* = \frac{m_{\mathrm{S}}}{a_{\mathrm{S}}} \cdot \delta(y - L_2) + \frac{a_y}{a_{\mathrm{S}}} \cdot k_1 \int_0^t c_y(\tau)\, \mathrm{d}\tau \tag{17}$$

The Eqs. (14)–(17) are the same as Eqs. (3)–(6) and the symbols have been determined in Section 6.1.

In addition, the overall deposition velocity V_{d} ($\mathrm{cm\,s^{-1}}$) and the reaction probability γ of the analyte on the solid material under study, have been defined earlier [86,114,115].

Finally, the necessary relations for calculating the values of ε, c_{max}^*, θ_i, $\varphi(\varepsilon)$ and β from Eq. (13), for the adsorption of gases on heterogeneous surfaces as a function of time, have been derived by combining (Eq. (13)) with Jovanovic isotherm model:

$$\theta(p, T, \varepsilon) = 1 - \exp(-Kp) \tag{18}$$

where

$$K = K^0(T) \exp\left(\frac{\varepsilon}{RT}\right) \tag{19}$$

R being the gas constant, and

$$K^0 = \frac{h^3}{(2\pi m)^{3/2}(kT)^{5/2}} \cdot \frac{\upsilon_{\mathrm{S}}(T)}{b_{\mathrm{g}}(T)} \tag{20}$$

Here, K is the Boltzmann's constant; m the molecular mass of the adsorbate, h the Planck's constant and the ratio

Table 9
Time distribution of adsorption energy, ε, local monolayer capacity, c^*_{max}, local adsorption isotherm, θ_i, energy distribution function, $\varphi(\varepsilon; t)$ lateral molecular interaction, β and gas equilibrium concentration c_y, for C_2H_6 on CaO at 323.2 K

t (min)	ε (kJ mol^{-1})	c^*_{max} (μmol g^{-1})	θ	$\varphi(\varepsilon; t)$ (cmol kJ^{-1} mol^{-1})	β	c_y (μmol cm^{-3})
4	88.51	0.174	0.572	9.111	1.665	2.657
6	88.98	0.252	0.215	6.287	0.210	4.307
8	90.33	0.540	0.481	9.290	0.011	5.152
10	92.24	0.793	0.621	8.761	−0.071	5.581
12	95.24	0.976	0.755	6.883	−0.046	5.783
14	102.7	1.065	0.927	2.503	−0.015	5.854
16	98.92	1.433	0.865	4.337	0.039	5.844
18	94.04	2.057	0.725	7.424	0.121	5.781
20	91.56	2.768	0.628	8.698	0.236	5.781
22	89.91	3.561	0.556	9.188	0.389	5.683
24	88.66	4.435	0.500	9.304	0.968	5.559
26	87.64	5.401	0.453	9.221	1.161	5.419
28	86.78	6.479	0.412	9.015	1.149	5.267
30	86.02	7.698	0.375	8.721	1.204	5.108
32	85.32	9.097	0.340	8.353	1.282	4.944
34	84.66	10.74	0.307	7.919	1.380	4.779
36	84.03	12.69	0.275	7.422	1.498	4.613
38	83.40	15.09	0.244	6.863	1.609	4.449
40	82.77	18.11	0.213	6.244	1.714	4.288
42	82.11	22.03	0.183	5.568	1.817	4.130
44	81.41	27.37	0.154	4.838	1.918	3.976
46	80.64	35.03	0.125	4.059	2.019	3.826
48	79.75	46.94	0.096	3.239	2.119	3.681
50	78.68	67.87	0.069	2.385	2.220	3.540
52	77.21	113.9	0.042	1.507	2.322	3.405
54	74.59	293.6	0.017	0.617	2.426	3.274
56	72.19	708.9	0.007	0.265	2.531	3.148
58	75.87	184.2	0.028	1.023	2.637	3.027
60	77.19	115.0	0.046	1.647	2.745	2.911
62	77.95	88.09	0.062	2.161	2.854	2.799
64	78.46	74.12	0.075	2.585	2.966	2.692
66	78.82	65.78	0.086	2.934	3.081	2.589
68	79.08	60.41	0.096	3.221	3.199	2.490
70	79.27	56.82	0.104	3.454	3.320	2.395
72	79.42	54.39	0.110	3.642	3.446	2.304
74	79.52	52.75	0.115	3.791	3.575	2.216
76	79.59	51.72	0.119	3.907	3.709	2.132
78	79.63	51.13	0.122	3.993	3.848	2.051
80	79.66	50.91	0.124	4.054	3.992	1.974
82	79.66	50.99	0.126	4.092	4.142	1.899
84	79.65	51.33	0.126	4.111	4.296	1.828
86	79.63	51.89	0.127	4.113	4.457	1.759
88	79.59	52.67	0.126	4.099	4.624	1.693
90	79.54	53.64	0.125	4.071	4.797	1.629
92	79.48	54.79	0.124	4.031	4.976	1.568
94	79.42	56.12	0.122	3.981	5.163	1.510
96	79.34	57.62	0.120	3.921	5.356	1.453
98	79.26	59.30	0.117	3.853	5.557	1.399
100	79.17	61.15	0.115	3.778	5.766	1.347
102	79.08	63.19	0.112	3.697	5.983	1.297
104	78.98	65.40	0.109	3.610	6.208	1.249
106	78.88	67.81	0.106	3.519	6.442	1.202
108	78.77	70.42	0.103	3.425	6.684	1.158
110	78.66	73.23	0.099	3.327	6.937	1.115
112	78.54	76.26	0.096	3.226	7.198	1.074
114	78.42	79.51	0.093	3.124	7.470	1.034
116	78.29	83.01	0.089	3.021	7.753	0.996
118	78.17	86.76	0.086	2.917	8.046	0.923
120	78.04	90.78	0.082	2.813	8.351	0.889
122	77.90	95.08	0.079	2.709	8.667	0.857
124	77.77	99.68	0.076	2.606	8.996	0.825

Table 9 (*Continued*)

t (min)	ε (kJ mol^{-1})	c^*_{max} (μmol g^{-1})	θ	$\varphi(\varepsilon; t)$ (cmol kJ^{-1} mol^{-1})	β	c_y (μmol cm^{-3})
126	77.63	104.6	0.073	2.503	9.337	0.794
128	77.49	109.9	0.069	2.402	9.691	0.765
130	77.35	115.5	0.066	2.302	10.06	0.737
132	77.20	121.5	0.063	2.204	10.44	0.710
134	77.06	128.0	0.060	2.108	10.84	0.684
136	76.91	134.8	0.057	2.014	11.25	0.659
138	76.76	142.2	0.055	1.923	11.68	0.634
140	76.61	150.0	0.052	1.834	12.12	0.611
142	76.45	158.4	0.049	1.747	12.58	0.588
144	76.30	167.3	0.047	1.664	13.06	0.567
146	76.14	176.9	0.045	1.583	13.56	0.546
148	75.99	187.1	0.042	1.504	14.07	0.526
150	75.83	198.0	0.040	1.429	14.61	0.507

From Ref. [113] with permission.

$\upsilon_S(T)$ /$b_g(T)$ of two partition functions, namely, that of the adsorbed molecule, $\upsilon_S(T)$, and that for rotations–vibrations in the gas phase $b_g(T)$. This ratio is taken as unity, approximately.

All parameters required refer to the values of $c_y(0, t)$, i.e. the concentration of the gaseous analyte at $y = 0$:

$$c_y(0,t) = \frac{\nu L_1}{D_z} \cdot c(l', t) = \frac{\nu L_1}{gD_z} \cdot \sum_{i=1}^{4} A_i \exp(B_i t) \tag{21}$$

where ν is the linear velocity of the carrier gas (cm s^{-1}) in the sampling column, L_1 the length of the diffusion column (cm) and D_z the diffusion coefficient of each gaseous analyte into the nitrogen carrier gas (cm^2 s^{-1}). From this, the value of the adsorbed concentration c^*_S is calculated

$$c^*_S = \frac{\alpha_y}{\alpha_S} \cdot k_1 \cdot \frac{\nu L_1}{gD_z} \cdot \sum_{i=1}^{4} \frac{A_i}{B_i} [\exp(B_i t) - 1] \tag{22}$$

Table 10
Standard errors of the pre-exponential factors $\ln A_i$ and the exponential coefficients B_i printed by the Lat-PC program for the system C_2H_6–CaO

	Values	Standard errors	r^2
$\ln A_1$	12.61	±0.03	0.999
$\ln A_2$	13.4	±0.9	
$\ln A_3$	13.086	±0.010	
$\ln A_4$	12.88	±0.04	
$\ln A_5$	12.656	±0.005	0.999
$\ln A_6$	12.3	±0.6	
$\ln A_7$	12.32	±0.11	
B_1	−0.01872	$\pm 2.4 \times 10^{-4}$	0.999
B_2	-8.6×10^{-2}	$\pm 1.0 \times 10^{-2}$	
B_3	-7.232×10^{-2}	$\pm 2.5 \times 10^{-4}$	
B_4	−0.3826	$\pm 4 \times 10^{-3}$	
B_5	-1.909×10^{-2}	$\pm 5 \times 10^{-5}$	0.999
B_6	−0.162	$\pm 2.2 \times 10^{-2}$	
B_7	−0.276	$\pm 1.5 \times 10^{-2}$	

From Ref. [113] with permission.

where the first fraction corresponds to the ratio of the cross-sectional area of the void diffusion column (cm^2) to the amount of solid under study per unit length of the same column (g cm^{-1}), k_1 is the local adsorption coefficient, and the rest of the symbols have been explained after Eq. (13).

The local adsorption isotherm is given by

$$\theta_t = \frac{c^*_S}{c^*_{max}} \tag{23}$$

where c^*_{max} is the local monolayer capacity, given by Eq. (24), and c^*_S is given by Eq. (22).

$$c^*_{max} = c^*_S + \frac{\partial c^*_S / \partial c_y}{KRT} \tag{24}$$

Thus, for the c^*_{max} determination the derivative $\partial c^*_S/\partial c_y$ and KRT from Eqs. (25) and (26), respectively, are needed:

$$\frac{\partial c^*_S}{\partial c_y} = \frac{a_y}{a_S} \cdot k_1 \cdot \frac{\sum_{i=1}^{4} A_i \exp(B_i t)}{\sum_{i=1}^{4} A_i B_i \exp(B_i t)} \tag{25}$$

$$KRT = \frac{gD_z}{\nu L_1} \times \left\{ \frac{\sum_{i=1}^{4} A_i B_i^2 \exp(B_i t)}{\left[\sum_{i=1}^{4} A_i B_i \exp(B_i t)\right]^2} - \frac{1}{\sum_{i=1}^{4} A_i \exp(B_i t)} \right\} \tag{26}$$

In all the above equations A_i and B_i are the pre-exponential factors and the exponential coefficients of Eq. (13).

More precisely, the relations for calculating ε (kJ mol^{-1}), c^*_{max} (mol g^{-1}) and θ_t from experimental data are given by Eqs. (27)–(29):

$$\varepsilon = RT[\ln(KRT) - \ln(RT) - \ln K^o] \tag{27}$$

$$c^*_{max} = c^*_S + \frac{1}{KRT} \cdot \frac{\partial c^*_S}{\partial c_y} \tag{28}$$

$$\theta_t = 1 - \frac{1}{c^*_{max}} \cdot \frac{1}{KRT} \cdot \frac{\partial c^*_S}{\partial c_y} \tag{29}$$

The probability density function $f(\varepsilon)$ of Eq. (12), on the other hand, describing the adsorption energy distribution, is defined as the derivative of the number of adsorption sites with respect to the adsorption energy [11,36]. Since the number of adsorption sites is proportional to the local monolayer capacity c^*_{max} of Eq. (28), $f(\varepsilon)$ may be defined as:

$$f(\varepsilon) = \frac{\partial c^*_{max}}{\partial \varepsilon} = \frac{\partial c^*_{max}/\partial t}{\partial \varepsilon/\partial t} \tag{30}$$

Finally one obtains [110]:

$$f(\varepsilon) = \frac{1}{RT} \cdot \left[\frac{KRT(\partial c^*_S/\partial t) + \partial^2 c^*_S/\partial c_y \partial t}{\partial(KRT)/\partial t} - \frac{\partial c^*_S/\partial c_y}{KRT} \right] \tag{31}$$

and from this the modified function $\varphi(\varepsilon)$ produced by multiplication of $f(\varepsilon)$ with θ followed by a division by c^*_{max} [111,112].

$$\varphi(\varepsilon; t) = \frac{\theta f(\varepsilon)}{c^*_{max}} \tag{32}$$

As regards the lateral interactions of the adsorbed molecules, the dimensionless parameter β [112] can be obtained:

$$\beta = \frac{z\omega}{RT} \tag{33}$$

ω being the lateral interaction energy and z the number of neighbors for each adsorption site. Thus, the $\theta z\omega$ is the added to ε differential energy of adsorption due to lateral interactions.

6.3. Theoretical analysis of kinetic physicochemical quantities

It is well known that the calculation of physicochemical parameters by the RF-GC method is based on a theoretical analysis of the diffusion band, obtained by plotting $H^{1/M}$ or $(1/M)\ln H$ against t, where H is the height or the area under the curve of the sample peaks, M the response factor of the detector (1 for FID) and t the time when the respective flow reversal was made. The theoretical analysis depends each time on the phenomena being studied and the mathematical model employed. In most cases it leads to the sum (or difference) of four, three or two exponential functions of time, describing the diffusion bands, i.e.

$$H^{1/M} = A_1 \exp(B_1 t) + A_2 \exp(B_2 t) + A_3 \exp(B_3 t) + A_4 \exp(B_4 t) \tag{34}$$

$$H^{1/M} = A_5 \exp(B_5 t) + A_6 \exp(B_6 t) + A_7 \exp(B_7 t) \tag{35}$$

The physical content of the pre-exponential factors A_1, A_2, A_3, A_4, A_5, A_6 and A_7 and the exponential coefficients of time B_1, B_2, B_3, B_4, B_5, B_6 and B_7, however is different each time, depending on the mathematical model used, which in turn depends on the physicochemical quantities being sought. For the present purpose the analysis was based on the solution of a system of partial differential equations comprising: (1) the mass balance equation for the gaseous analyte being studied in the gaseous region z of the diffusion column (cf. Fig. 3); (2) the mass balance equation of A in region y, filled with the solid under study; (3) the rate of change of the concentration of the analyte A adsorbed on the solid surface; (4) the definition of the local adsorbtion isotherm, describing the relation between gaseous and adsorbed concentration of A in region y. This general definition of the isotherm equation suffices, so that the real experimental isotherm is automatically incorporated into the final calculations.

The auxiliary parameters X, Y, Z and W are first calculated [94]:

$$X = \alpha_2(1 + V_1) + 2k_{app} + k_{-1} + k_2 = -(B_1 + B_2 + B_3 + B_4) \tag{36}$$

$$Y = [\alpha_2(1 + V_1) + 2k_{app}](k_{-1} + k_2) + \alpha_1\alpha_2 + k_1k_{-1} + k^2_{app} + \alpha_2(1 + V_1)k_{app} = B_1B_2 + B_1B_3 + B_1B_4 + B_2B_3 + B_2B_4 + B_3B_4 \tag{37}$$

$$Z = \alpha_1\alpha_2(k_{-1} + k_2) + \alpha_2V_1k_1k_{-1} + k_1k_{-1}k_2 + \alpha_2(1 + V_1)(k_{-1} + k_2)k_{app} + k_1k_{-1}k_{app} + k^2_{app}(k_{-1} + k_2) = -(B_1B_2B_3 + B_1B_2B_4 + B_1B_3B_4 + B_2B_3B_4) \tag{38}$$

$$W = (\alpha_2V_1 + k_{app})k_1k_{-1}k_2 = B_1B_2B_3B_4 \tag{39}$$

where B_1, B_2, B_3 and B_4 are the exponential coefficients of time in Eq. (34), by means of which the auxiliary parameters X, Y, Z and W are calculated. The physicochemical parameters k_1, k_{-1}, k_2 and k_{app}, appearing in Eqs. (36)–(39) are defined as follows: k_1 is the local adsorbtion parameter for the analyte pollutant A (s^{-1}); k_{-1} the desorption rate constant of A from the solid surface (s^{-1}); k_2 the rate constant of a possible first- or pseudofirst-order surface reaction of the adsorbed analyte A (s^{-1}); k_{app} the apparent first-order rate constant of a chemical reaction of A with another substance B in the gaseous phase above the solid; $\alpha_1 = 2D_1/L^2_1(s^{-1})$, D_1 being the diffusion coefficient ($cm^2\,s^{-1}$) in section z, and $\alpha_2 = 2D_2/L^2_2(s^{-1})$, D_2 being the diffusion coefficient ($cm^2\,s^{-1}$) in section y; and the dimensionless volume V_1 by:

$$V_1 = \frac{2V'_G(empty)\varepsilon}{V_G} + \frac{\alpha_1}{\alpha_2} \tag{40}$$

L_1 and L_2 being the lengths of the sections z and y of the diffusion column, respectively, V_G and V'_G their gaseous volumes and ε the external porosity of the solid bed.

A steady-state assumption for the adsorbed concentrations leads to Eq. (35). Instead of Eqs. (36)–(39), the following relations are valid:

$$X_1 = \alpha_2(1 + V_1) + 2k_{app} = -(B_5 + B_6 + B_7) \tag{41}$$

$$Y_1 = \alpha_1\alpha_2 + \frac{k_1k_{-1}k_2}{k_{-1}+k_2} + \alpha_2(1+V_1)k_{app} + k_{app}^2 = B_5B_6 + B_5B_7 + B_6B_7 \quad (42)$$

$$Z_1 = \frac{(\alpha_2V_1 + k_{app})k_1k_{-1}k_2}{k_{-1}+k_2} = -(B_5B_6B_7) \quad (43)$$

Using non-linear regression analysis personal computer programmes available from the authors, one can calculate the exponential coefficients of time B_1, B_2, B_3, B_4, B_5, B_6 and B_7, and from them the auxiliary parameters X, Y, Z, W, X_1, Y_1 and Z_1. Through these, with the help of Eqs. (36)–(43), k_1,k_{-1}, k_2, k_{app} and α_1 are computed. The α_2 value is calculated in another experiment, using only A in the absence of a second substance B, when $k_{app} = 0$ in all Eqs. (36)–(43). Finally, the overall deposition velocity V_d (cm s^{-1}) and the reaction probability γ of the analyte A on the solid material under study are found by the relations

$$V_d = \frac{k_1V'_G(empty)\varepsilon}{A_S} \cdot \frac{k_2}{k_{-1}+k_2} \quad (44)$$

$$\frac{1}{\gamma} = \left(\frac{R_gT}{2\pi M_B}\right)^{1/2} \cdot \frac{1}{V_d} + \frac{1}{2} \quad (45)$$

where A_S is the total surface area of solid (cm^2), R_g the ideal gas constant (J K^{-1} mol^{-1}), M_B the molar mass of analyte A (kg mol^{-1}) and T the absolute temperature, K.

6.4. Experimental section for the reversed-flow gas chromatography method

The RF-GC technique involves a flow-rate pertubation of the carrier gas which is achieved experimentally simply by using a four- or six-port gas sampling valve and reversing the direction of flow of the carrier gas, usually for a short time interval. If pure carrier gas passes through the sampling column, nothing happens on reversing the flow. If a solute comes out of the diffusion column at $z = 0$ (cf. Fig. 3) as the result of its diffusion into the carrier gas, filling the column z and also running along the sampling column, the flow reversal records the concentration of the solute at the junction of the sampling column with that of the diffusion one, at the moment of the reversal. This concentration recording has the form of extra chromatographic peaks superimposed on the otherwise continuous detector signal (cf. Fig. 5). The moment of injection is the time 0.

The chromatograph used was a Shimadzu 8A, slightly modified, with an FID detector. The experimental arrangement (cf. Fig. 3) was analogous to that used in catalytic studies [114,126], which is very different from the others used in the past (cf. Fig. 4) [86,92,114,115]. Here, the L_1 section (20.5–23.4 cm) did not contain any solid material, while the L_2 (4.0–5.0 cm) contained the solid bed. Both sections L_1 and L_2 were of Pyrex glass of I.D. 3.5 mm. The sampling column $l' + l$ (40 cm + 40 cm) was a stainless steel chromatographic tube of 4.0 mm I.D.

Adsorbents were packed in columns made from Pyrex glass. Before the adsorption experiments, the column with the adsorbate was conditioned at 473 K for 24 h under a flow of nitrogen, followed every time by the adjustment of the working temperature. The flow-rate measured at the outlet of the column was constant and equal to about 26 cm^3 min^{-1}.

The conditioning of the solid bed by heating it at 473 K for 24 h under a continuous carrier gas flow is a necessary work. After that the bed was cooled to the working temperature. Then 1 cm^3 for example of hydrocarbon was introduced through the injector at $y = L_2$. In the experiments with O_3 or NO_2, 0.2 cm^3 of O_3 (NO_2) was injected after the injection of 0.5 cm^3 of hydrocarbon and after that another 0.5 cm^3 of the hydrocarbon was introduced into the system.

As regards the experiments with liquids, a small quantity of the liquid (e.g. 4×10^{-3}cm^3 benzene or toluene) was injected through the end of column L_2 with 0.2 cm^3 of O_3 or gaseous nitrogen dioxide at atmospheric pressure, and, after the appearance of the continuously rising concentration–time curve, the reversing procedure for the nitrogen carrier gas flow started, each reversal lasting always 10 s. This is shorter than the gas hold-up time in section l and l' of the sampling column.

Repeated flow reversals of the carrier gas flowing only through the sampling column can be made, by means of the four port-valve. The narrow fairly symmetrical sample peaks (cf. Fig. 5) created by the flow reversals, were recorded and their height was printed as a function of time t. This procedure was done automatically by using an electronic valve. The narrow fairly symmetrical sample peaks created by the flow reversals were stored in a personal computer by using the CLASS VP chromatography data system. Finally, they were printed, by using an ink-jet printer. This was done first for the gas (hydrocarbon) only and secondly for any binary system (hydrocarbon/O_3).

The plot of ln H versus experimental time is the diffusion band (cf. Fig. 6). Through the slope of these diffusion bands all the physicochemical quantities required are determined.

6.5. Experimental results and discussion of single gas adsorption isotherms

In Table 1 the differential isotherms and the integrated ones for PbO and two aromatic hydrocarbons are shown, while the integrated isotherms for this adsorbent as well as for three others are plotted and shown in Fig. 7.

In Table 2, the differential and the integrated isotherms of Ethene on Penteli marble are presented. The difference between the two Tables is that in the latter the experimental set-up used was that of Fig. 4 instead of Fig. 3 corresponding to the first case.

From these representative results, it is obvious that a characterization of the adsorptive properties of the different solids is possible. It is shown for example that PbO has a much different behavior from the other oxides used (cf. Fig. 7). That is, among TiO_2, Cr_2O_3, Fe_2O_3, and PbO

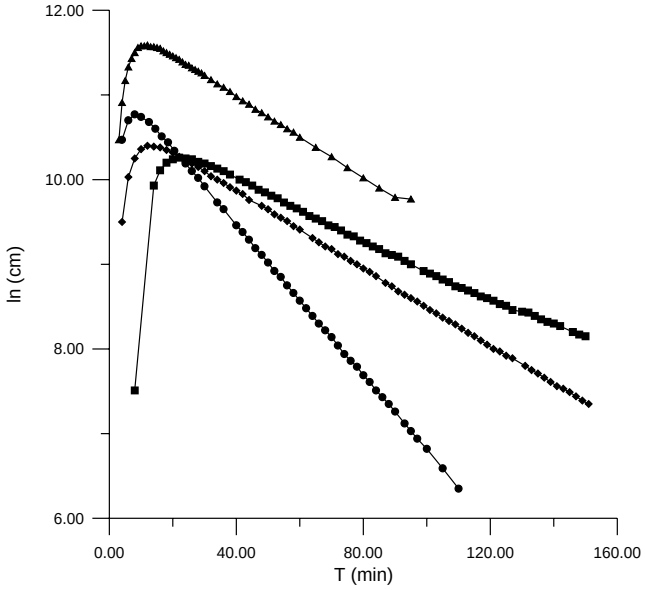

Fig. 6. Diffusion bands at 313.2 K (from Ref. [84] more precisely Fig. 3 of this with permission) of: (◆) 1 cm^3 C_2H_4 injected in a γ-Al_2O_3 denuderl; (■) 1 cm^3 C_2H_2 injected in a γ-Al_2O_3 denuder; (▲) 1 cm^3 C_2H_4 injected in a void diffusion column; (●) 1 cm^3 C_2H_2 injected in a void diffusion column.

studied with benzene or toluene, the isotherms of the last oxide have the lower c_S^* values. The shapes of all isotherms remain unchanged. All the above lead to very different values of the physicochemical constants determined, among which the deposition velocity and the reaction probability are the highest [91,93–95].

It is obvious that one can conclude safely and accurately about chemical reactivity (cf. Table 3).

An analogous behavior appears when the lead oxide is studied in the presence of aliphatic hydrocarbons. With the exception of ethyne, all the other systems, i.e. C_2H_6–PbO, C_3H_6–PbO, 1-C_4H_8–PbO and even C_2H_4–PbO display c_S^* values up to $(1.2–16) \times 10^{-8}$ mol g^{-1}. The C_2H_2–PbO system exhibits much higher c_S^* values, while the iron oxide covers a distance from $(0.002 \times 10^{-8}$ to 12×10^{-8} mol g^{-1} for the same hydrocarbons.

We believe that this method is to be preferred compared to the classical inverse gas chromatographic methods, which are elution techniques. This method has the following advantages [83]: (1) it does not need an a priori isotherm equation; (2) it accounts for the mass transfer phenomena; (3) it takes into account desorption; (4) a sorption effect is absent; (5) it produces isotherms in the presence of a possible heterogeneous and also an homogeneous reaction in the gas-phase.

In addition, further advances were achieved recently: (a) explicit calculation of the isotherms was not carried out as described in Ref. [83] but was based on further improved equations [79]; (b) the adsorption and kinetic measurements were rendered independent of the diffusion coefficient of the gas injected, which until then was determined independently, found in the literature or calculated theoretically, under different conditions, and used for the kinetic calculations; (c) the experimental set-up does not include a denuder tube as in the previous works, but a diffusion column containing the solid adsorbent or an ordinary catalytic bed. This arrangement was first used in Ref. [116] but the results were based on linear isotherms.

For all these reasons, the results based on this new arrangement and the improved mathematical model of a non-linear adsorption isotherm are accurate. The present method gives accurate values of the kinetic constants studied [94,95], because of the non-linear model isotherm calculation, helped by the use of a suitable personal computer program, as the non homogeneity of the surface of the oxides studied here does not permit a linear adsorption isotherm model [88]. A point worth mentioning is that comparison of these isotherms with others measured by established methods is impossible, since in the present case we are dealing with local isotherms, with each value referring to a particular adsorption energy changing with time, whilst those based on traditional methods are global overall isotherms. Ideed, RF-GC gives $\{\theta(p, T, \varepsilon)\}$ while $\{\Theta(p, T)\}$ is measured conventionally.

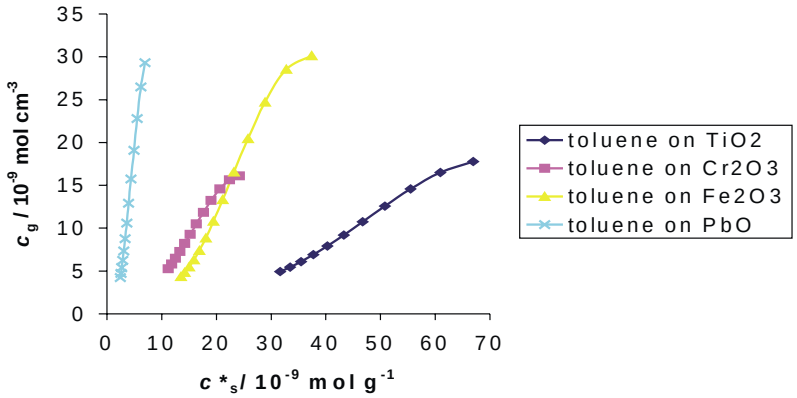

Fig. 7. Adsorption isotherms for PbO, Fe_2O_3, TiO_2, Cr_2O_3 with toluene. From Ref. [79] with permission.

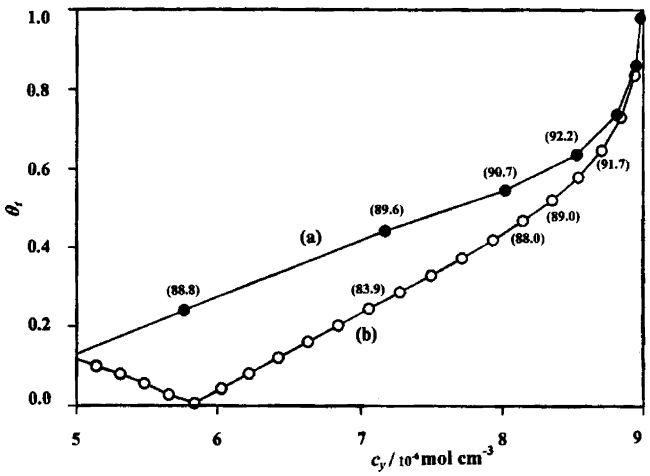

Fig. 8. Adsorption–desorption isotherm plots at 323.2 K for the system C_3H_6/PbO in a nitrogen atmosphere. Numbers in parenthesis are the energies of adsorption in kJ mol^{-1}. From Ref. [109] with permission.

Furthermore, another evidence that θ_t represents a local isotherm is its plot as a function of c_y in Fig. 8. It looks like a hysteresis loop of adsorption, but it is not, since the desorption (b) curve lies below that of adsorption (a). The latter corresponds to the ascending branch of Fig. 6, while desorption is connected with the descending branch of c_y {cf. Fig. 12c in this review, and Fig. 2d in Ref. [109]}. The separation of the desorption (b) from the adsorption (a) curve is most probably due to irreversible adsorption of the adsorbate on the solid surface. The extent of irreversibly adsorbed analyte can be calculated as described elsewhere [83]. The magnitude range of the adsorption energies points to a rather regular distribution model for the adsorption sites on heterogeneous surfaces, in the domain of chemisorption. The adsorption energy increasing with θ_t up to a maximum close to unity for the latter confirms that different collections of adsorption sites are involved at different times.

6.6. Gas chromatographic determination of binary adsorption isotherms

Gas chromatography in contrast to static methods is of considerable interest for studying adsorption at finite surface coverage, because it readily allows measurements over a wide range of temperature [117]. This technique provides a means to determine the adsorption isotherms from which the surface area, porosity and surface energy [85,118] are determined. When adsorption takes place at finite surface coverage the isotherms are generally non-linear and hence retention volumes are dependent upon the adsorbate concentration in the gas phase. In addition, a non-linear isotherm leads to asymmetrical peaks, the shape of which and the retention time being dependent on the volume injected.

The majority of papers devoted to single-gas adsorption assumed that the surface of the adsorbent is homogeneous; however, single-gas adsorption systems with adsorbate molecules of complex chemical structure and adsorbents of complex chemical composition and porous structure cannot be described by means of equations derived for homogeneous surfaces [36]. Thus, for these more complex systems, surface heterogeneity plays an important role and must be taken into account in the physicochemical interpretation of the adsorption process [83]. Various forms of perturbation chromatography have been used to measure pure-component isotherms and in a few cases binary isotherms.

Gas–solid equilibrium isotherms of binary and more complex systems are of significant theoretical and practical interest. However, the experimental difficulties for complex systems have led to limited data available compared to the immense amount of information data and models available for single-component adsorption systems [119].

In [89], a case study concerning binary gas–solid experimental adsorption isotherms are presented using the technique and the methodology of the RF-GC. This method is a well known perturbation chromatographic one combining the simplicity with the accuracy used recently in studying physicochemical constants in homogeneous gas phase [120,121] and in heterogeneous as well [84,87,94,95].

RF-GC is a dynamic method useful for measuring adsorption isotherms at low concentrations. This method based on the mass–balance equations is useful for evaluating the adsorption isotherms because it gives model-independent results. The method is described and evaluated for the determination of the adsorption isotherms of two components in gas–solid systems. The following adsorbents were included in this case study [89]: iron oxide, zinc oxide, chromium oxide, lead oxide and titanium oxide. The adsorption of two significant aromatic hydrocarbons (benzene and toluene) was investigated in the presence of an inorganic gas (nitrogen dioxide).

6.7. Results and discussion of binary adsorption isotherms

Usually in the studies of physical adsorption on heterogeneous surfaces, the following procedure is applied: the energy distribution function is evaluated from an overall adsorption isotherm given in an analytical or tabulated form, from experimental adsorption data [36]. Thus, the existence of such a Table is valuable for studying the surface energy distribution.

Some representative results concerning binary adsorption isotherms are presented in Table 4 {from Ref. [90]} and in Figs. 9 and 10 {from Ref. [89]}, respectively. Table 5 demonstrates simple and binary adsorption isotherms for 10 heterogeneous systems.

The simultaneous adsorption equilibrium of a binary gas mixture on a solid surface can be described by three variables: $\partial c_S^*/\partial c_y$, c_S^* and c_y (or c_G). Thus, two types of isotherms are used for the description of adsorption equilibrium: the *differential* and the *integral* one. Both are tabulated for example in Tables 2–6 of Ref. [89] (first and second column respectively) with the corresponding values of c_y. From these tables, it is seen that the adsorbed

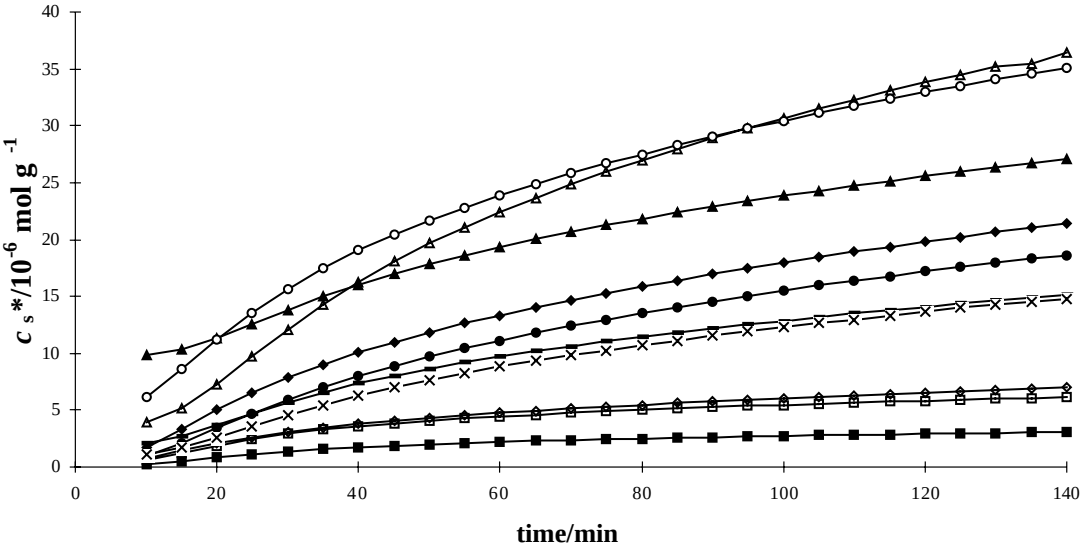

Fig. 9. Binary adsorption isotherms of pure benzene and of benzene–nitrogen dioxide on the five solids, {from Ref. [89] with permission, Fig. 3} as follows: (C_6H_6–NO_2–ZnO, C_6H_6–ZnO); (C_6H_6–NO_2–Cr_2O_3, C_6H_6–Cr_2O_3); (C_6H_6–NO_2–PbO, C_6H_6–PbO); (C_6H_6–NO_2–TiO_2, C_6H_6–TiO_2); (C_6H_6–NO_2–Fe_2O_3, C_6H_6–Fe_2O_3).

amount c_S^* is not a unique function of the gas phase concentration c_y, as expected from an ordinary conventional adsorption isotherm. It seems as that a single partial pressure corresponding to c_y, can produce two different surface coverage at some areas. This behavior stems from the fact that Eq. (3) does not give the total monolayer coverage of the entire homogeneous surface, but it is a *local adsorption* equation for a heterogeneous surface, sweeping it over the various active sites of different adsorption energy with time. It is a usual experimental finding for c_y to increase with time initially, pass over a maximum and then decrease exponentially with time. Two different times may exhibit the same value for c_y, one in the ascending branch and the other in the descending one. But these do not correspond to the same value for the adsorbed concentration c_S^*, since different kinds of adsorption sites contribute to the adsorption process in the two above cases, i.e. at two different times. It follows that isotherm graphs similar to the conventional

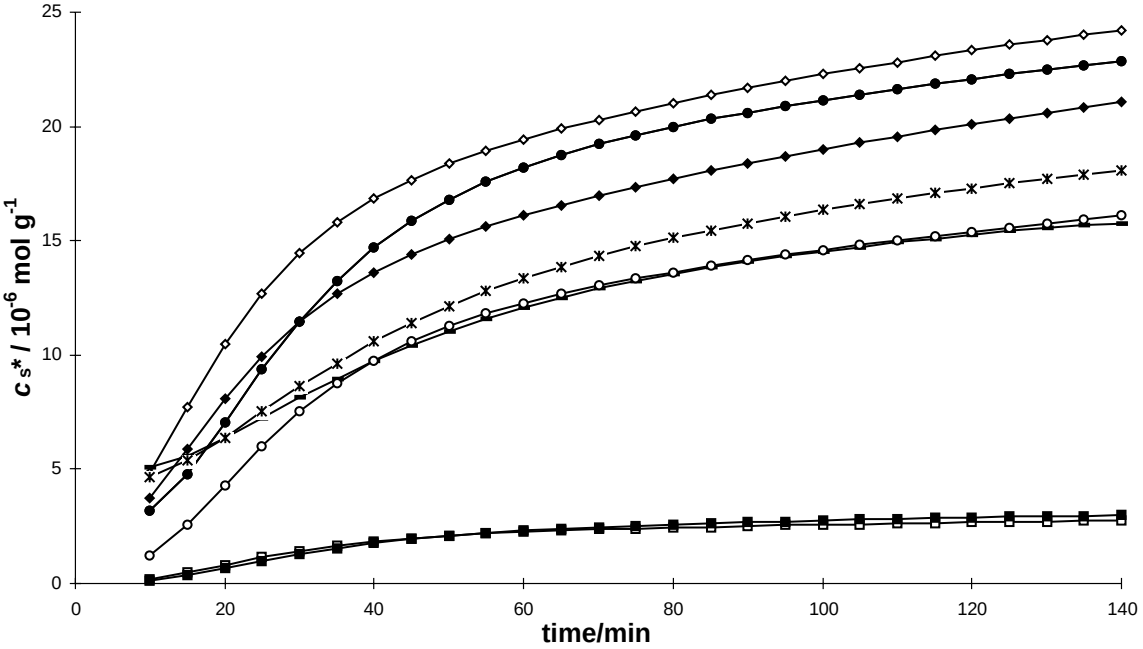

Fig. 10. Binary adsorption isotherms of pure toluene and of toluene–nitrogen dioxide on four solids, {from Ref. [89] with permission, Fig. 5} as follows: (C_7H_8–NO_2–ZnO, C_7H_8–ZnO); (C_7H_8–NO_2–Cr_2O_3, C_7H_8–Cr_2O_3); (C_7H_8–NO_2–PbO, C_7H_8–PbO); (C_7H_8–NO_2–Fe_2O_3, C_7H_8–Fe_2O_3).

ones can be obtained by plotting c_S^* as a function of time. Figs. 9 and 10 give some examples.

In these figures the pure-aromatic isotherms as well as the binary aromatic hydrocarbon—nitrogen dioxide ones on the same oxides are presented. The only experimental difference between pure aromatics and binary adsorptions is the presence of nitrogen dioxide in the latter ($v_{\text{hydrocarbon}}/v_{NO_2} = 20$).

In six systems: C_6H_6–NO_2/PbO, C_6H_6–NO_2–TiO_2, C_6H_6–NO_2–Fe_2O_3, C_7H_8–NO_2–TiO_2, C_7H_8–NO_2–ZnO and C_7H_8–NO_2–Cr_2O_3, a displacement to higher adsorption values, as compared with the respective pure aromatic compounds, is noted, under the same experimental conditions. In three other cases: C_7H_8–NO_2–Fe_2O_3, C_6H_6–NO_2–ZnO and C_6H_6–NO_2–Cr_2O_3, the displacement is opposite, i.e. to lower values. Finally, the systems: C_7H_8–NO_2–PbO and C_7H_8–PbO show about the same adsorption isotherms.

Among TiO_2, Fe_2O_3, Cr_2O_3, ZnO and PbO studied with benzene or toluene in the presence of nitrogen dioxide, the isotherm of the last oxide with benzene has the smallest values of c_S^*, while the TiO_2 has the highest. The shape of the isotherms remains always unchanged. The maximum value for c_y corresponding to a certain c_S^* may be due to a completion of a monolayer of adsorbed molecules. Further increase of c_S^* can be interpreted as due to multilayer adsorption, causing a decrease in c_y [83]. All the above lead to very different values of the physicochemical constants determined, among which the deposition velocity and the reaction probability are the highest [84,94,95].

It is believed that RF-GC offers a simple way to draw safe and accurate conclusions about chemical reactivity of many systems, which can be investigated with the RF-GC method based on these experimentally obtained isotherms.One can see that the present method gives accurate values of the kinetic constants studied (cf. Tables 6–7), [94,95] including a non-linear model isotherm calculation, with a suitable personal computer program. Non-homogeneity of the surface, like that of the oxides studied does not permit a linear adsorption isotherm model.

Thus, one can conclude safely and accurately about chemical reactivity and kinetics [89,90] and give correct explanations for the systems examined and many other based on these experimentally obtained isotherms. The reason is that kinetic parameters are closely related to the existing adsorption isotherm, depending strongly on the adsorption–desorption phenomena. Thus, some representative kinetic constants namely: the dynamic adsorption rate constants (k_1), the desorption rate constants (k_{-1}), the surface reaction rate constants (k_2) for five aliphatic hydrocarbons in the presence of NO_2 are presented in Tables 6–7. The two squared correlation coefficients denoting the goodness of curve fitting of the four and the three exponential equations of the improved mathematical model used, are presented also.

In all kinetic experimental results obtained by RF-GC, which have been published the squared correlation coefficient r^2 was in the range 0.9–0.999, (and in most cases in the range 0.991–0.999) presenting a remarkable goodness of fit for a non-linear regression analysis. The $\langle t \rangle$ test of significance for the smallest r^2 found, shows that is highly significant, with a probability to be exceeded smaller than 0.05%. These coefficients, which in addition to the reasons given below, permit us to reinforce the validity of this method. The same personal computer program [94] can also print the values of the exponential coefficients together with their standard errors (cf. Table 8). The errors found in all runs carried out in the works mentioned above are reasonable for physicochemical constants.

6.8. Comparison of the reversed-flow gas chromatography with other methods

A complete statistical description of real multi-component adsorption systems is still a unsolved problem. Thus, applications of this treatment for characterization of real adsorption systems and prediction of adsorption from multicomponent mixtures is impossible at present; in addition, the further complication introduced through the heterogeneity of the surface makes a full statistical thermodynamic treatment untenable [36].

Of the classical methods for measuring adsorption, only volumetric methods have been used to measure binary adsorption equilibrium [122]. These methods lack the speed precision and temperature range of the RF-GC method.

When using the elution method (the best one among the older GC methods) to obtain the adsorption isotherms, the sorption effect, that is to say, the change in gas flow-rate caused by the sorption or desorption of the solute molecules in the stationary phase causes the greatest error in the isotherm determination [122,123].

In the RF-GC method the sorption effect is non-existent. Besides this method has the following advantages [83,94,95, 124,125]:

(1) the diffusion and resistance to mass transfer are not neglected;
(2) pressure gradient is negligible along the bed;
(3) it leads directly to an experimental isotherm without specifying a priori an isotherm equation;
(4) the isotherm can be determined in the presence of a surface reaction of the adsorbate;
(5) it is simple and fast;
(6) it has an acceptable accuracy.

6.9. Calculations of the energetic physicochemical quantities (adsorption energy, ε, local monolayer capacity, c_{max}^*, local adsorption isotherm, θ_t, energy distribution function, $\varphi(\varepsilon)$, and lateral interaction energy, β)

Reversed-flow gas chromatography is extended to the measurements of the probability density function for the adsorption energies as well as the differential energies of adsorption due to lateral interactions of molecules adsorbed

on different heterogeneous solid surfaces. All these calculations are based on a non-linear adsorption isotherm model as it is well accepted that the linear one is inadequate for substances such as these used in practical applications. Thus, some new important physicochemical parameters have been obtained for the characterization of the heterogeneous systems studied [113,126,127]. The adsorbents used were calcium oxide, magnesium oxide or Penteli marble. The adsorption of many significant hydrocarbons was investigated.

Table 9 shows some representative results, while in Table 10 the standard errors of the pre-exponential factors and the exponential coefficients responsible for the estimation of values in Table 9 are presented.

The calculations of the energetic physicochemical quantities ε, c^*_{max}, θ_t, $\varphi(\varepsilon)$ and β pertaining to heterogeneous surfaces, start from the diffusion bands of RF-GC experiments (cf. Fig. 6 of this review or Fig. 3 of Ref. [92]) by recording the pairs H, t and calculating the pre-exponential factors A_1, A_2, A_3 and A_4, and the time coefficients B_1, B_2, B_3 and B_4. By entering the pair values of H, t into the DATA lines of a non-linear regression analysis GW- PC programme, together with the other unknown quantities in the INPUT lines, the physicochemical parameters and functions exposed and defined in Section 6.2. are calculated and printed. These calculations are based on the Jovanovic local isotherm model. It should be stressed that the relations given in the Section 6.2. describe all the quantities ε, c^*_{max}, θ_t, $\varphi(\varepsilon)$ and β as analytic functions of time.

Figs. 11–16 plot graphically ε, θ_t, $\varphi(\varepsilon)$, β θ_t, and c_y, as functions of time, using suitable software (e.g. Excel). Thus, a time resolved analysis was performed. All the maxima and minima observed are appeared before a steady state establishment. On the other hand, in the same Figures θ_t and $\varphi(\varepsilon)$ are plotted versus adsorption energy ε. More precisely, the six Figures mentioned above presented:

- Fig. 11a: plots of distribution function $\varphi(\varepsilon; t)$ against adsorption energy values ε, for C_2H_6, on CaO at 323.2 K;
- Fig. 11b: plots of distribution function $\phi(\varepsilon; t)$ as a function of time, for C_2H_6, on CaO at 323.2 K;
- Fig. 11c: plots of the lateral molecular interaction energy $\beta\theta_i$ (dimensionless) as a function of time for C_2H_6, on CaO at 323.2 K;
- Fig. 12a: plots of local adsorption energy ε, as a function of time for C_2H_6, on CaO at 323.2 K;
- Fig. 12b: plots of local adsorption isotherm θ_i as a function of time for C_2H_6, on CaO at 323.2 K;
- Fig. 12c: plots of gaseous adsorbate concentration c_y as a function of time for C_2H_6 on CaO at 323.2 K.

In Figs. 13–16, an analogous behavior for two others gases, with the same adsorbent is presented.

Some curves show an initial and a final part which deviate from the main experimental part. Most of the experimental measurements fall on the same curve, irrespective whether they correspond to the ascending or the descanding branch of the c_y versus t curve. Thus, the local isotherm values

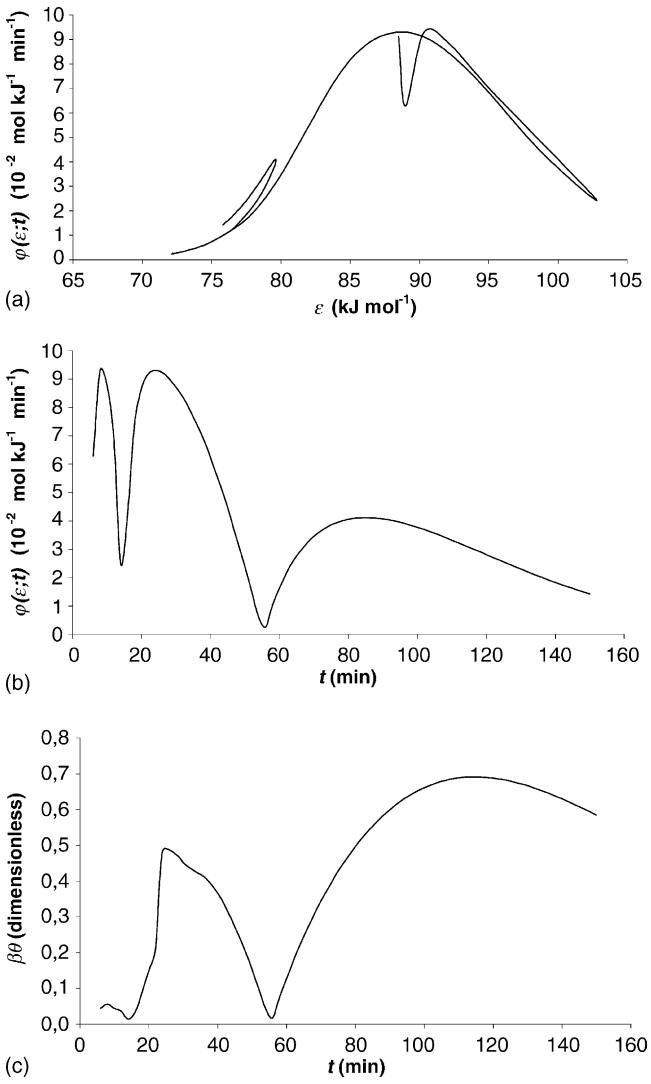

Fig. 11. Plots of: (a) distribution function $\varphi(\varepsilon; t)$ against adsorption energy values ε, (b) distribution function $\varphi(\varepsilon; t)$ as a function of time, and (c) the lateral molecular interaction energy $\beta\theta_i$ (dimensionless) as a function of time for C_2H_6, on CaO at 323.2 K. From Ref. [113] with permission.

depend strictly on the adsorption energy value, irrespective of the time when this was measured. The shape of these curves resembles that given by Adamson and Ling [23], as exemplified by Rudzinski and Everret [11]. The big difference is that in this case all the physicochemical quantities are obtained experimentally and not analytically [11,36]. As regards the comparison of the energy distribution function versus time, in this work and in Bakaev and Steele [128],one can see a similarity with the exception that our first is an experimental one, while that of Bakaev and Steele coming through simulation. As regards, on the other hand, the comparison of the energy distribution function versus energy of adsorption, the shape of the curves is always a Gaussian, also experimental.

From all figures in Ref. [113], a different behavior for the different heterogeneous systems is observed. Thus,

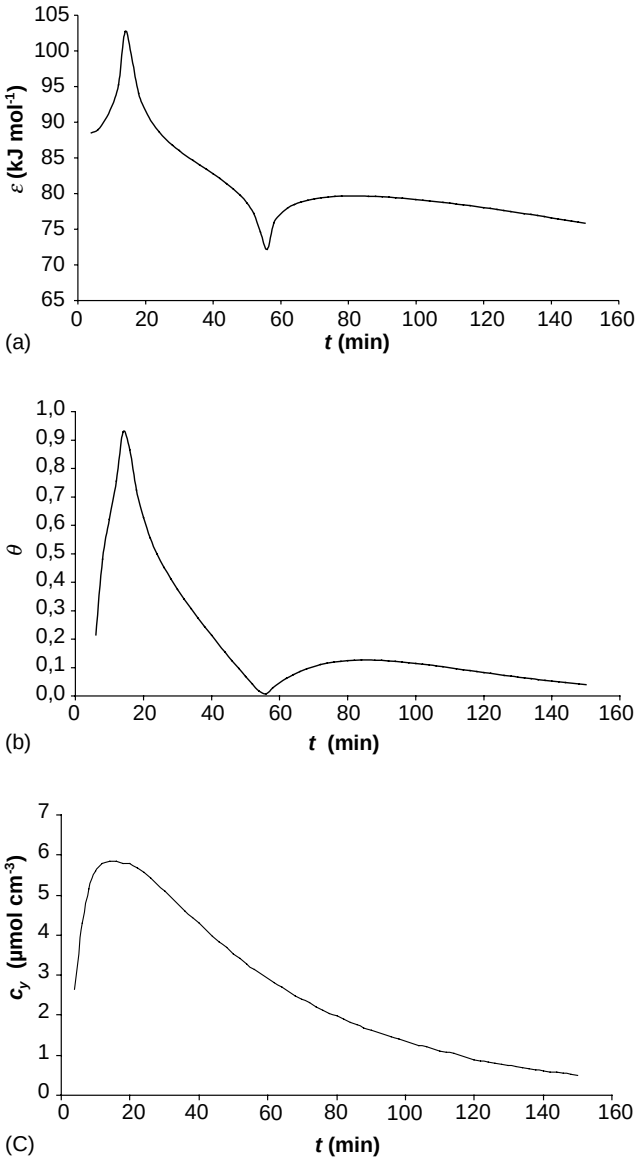

Fig. 12. Plots of: (a) local adsorption energy ε, (b) local adsorption isotherm θ_i and (c) gaseous adsorbate concentration c_y as a function of time for C_2H_6 on CaO at 323.2 K. From Ref. [113] with permission.

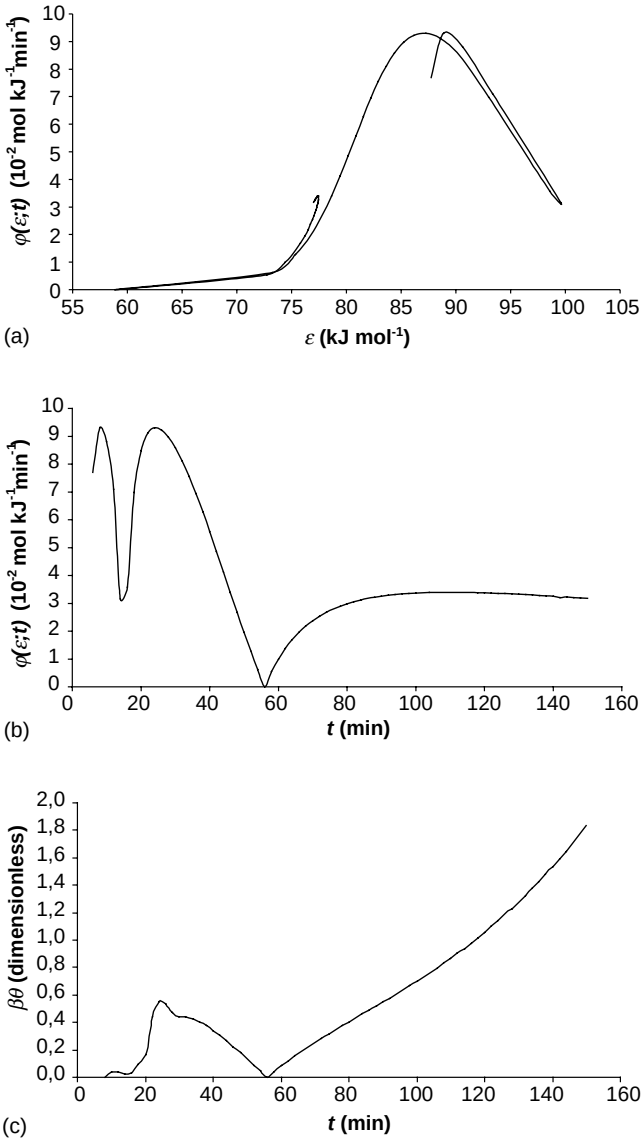

Fig. 13. Plots of: (a) distribution function $\varphi(\varepsilon; t)$ against adsorption energy values ε, (b) distribution function $\varphi(\varepsilon; t)$ as a function of time, and (c) the lateral molecular interaction energy $\beta\theta_i$ (dimensionless) as a function of time for C_2H_4, on CaO at 323.2 K. From Ref. [113] with permission.

with a simple inverse gas chromatographic technique, some very important for the surface chemistry quantities can be determined for the solid study and characterization, especially when heterogeneous surfaces are under investigation. Then, all above local quantities are determined from the experimental H, t pairs by a nonlinear least-squares method, through some suitable relations mentioned above in Section 6.2.

6.10. Advantages of the reversed-flow gas chromatography method

Adsorption isotherms and surface energy distribution functions on heterogeneous surfaces have been the subject of many efforts during the last two decades for characterizing heterogeneous solids by calculating adsorption energy distribution functions from retention volume data. All these works offer approximate functions or values through approximate solutions without any determination of the actual values of adsorption parameters [36].

Of all the classical methods for measuring adsorption energies, isotherms etc. none has led to local values. These methods lack the precision and the possibility of the RF-GC method. Difficulties like these led scientists to turn to numerical solutions [85,89,117,118].

The RF-GC method has the following advantages [83,89]: (1) it is simple and fast; (2) it is accurate; (3) the diffusion and resistance to mass transfer are taken into account

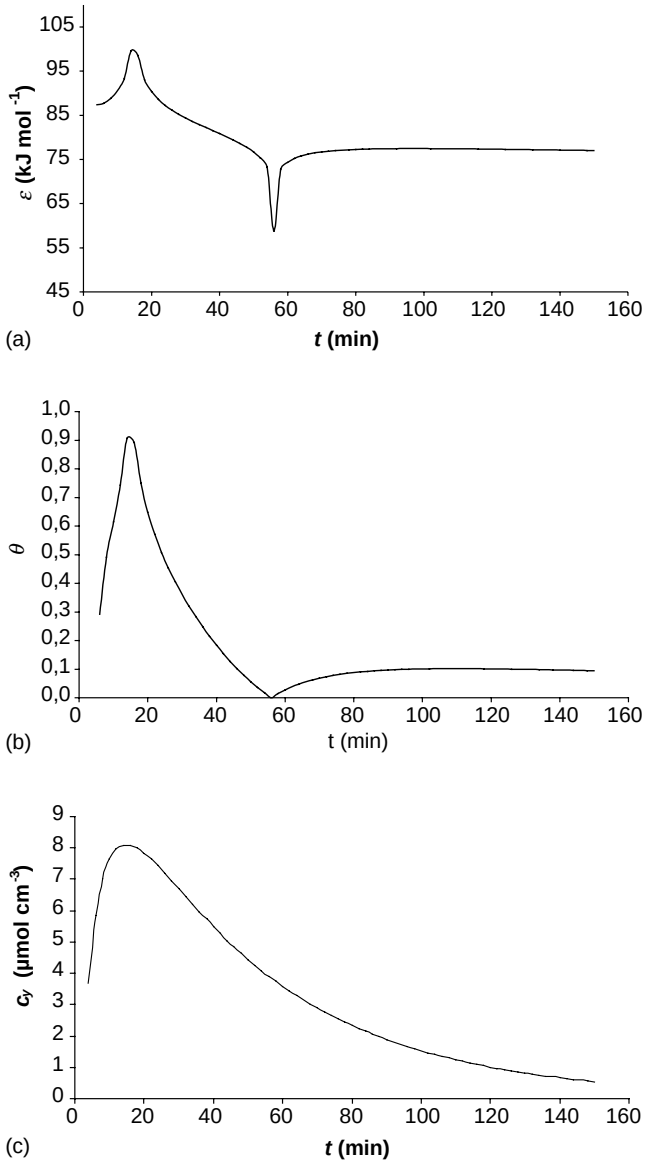

Fig. 14. Plots of: (a) local adsorption energy ε, (b) local adsorption isotherm θ_i and (c) gaseous adsorbate concentration c_y as a function of time for C_2H_4 on CaO at 323.2 K. From Ref. [113] with permission.

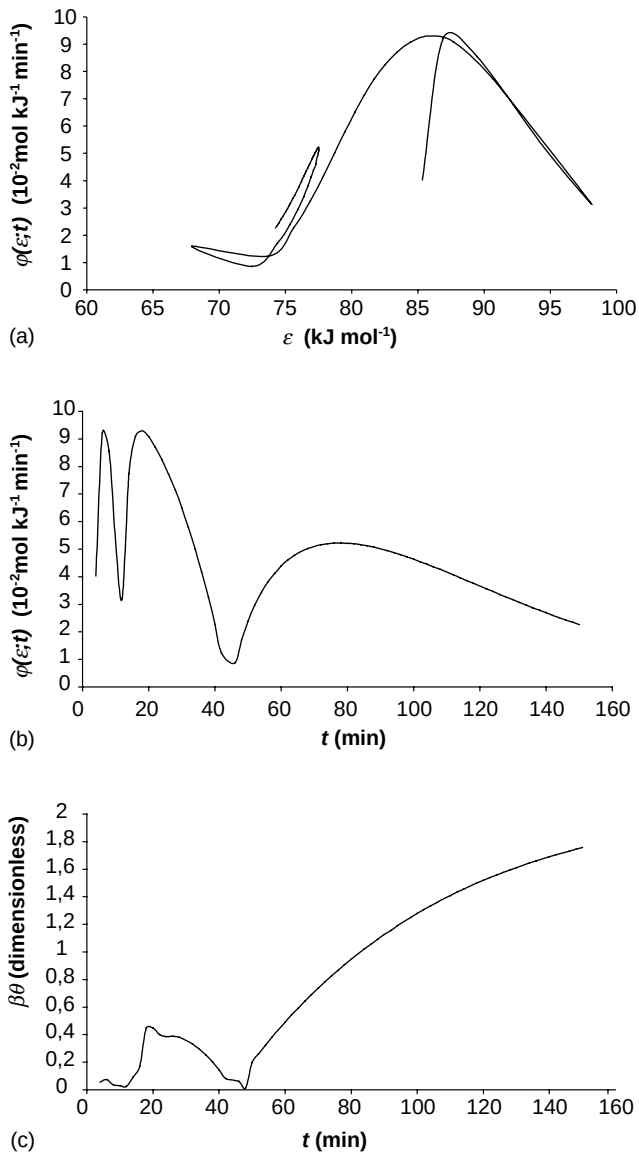

Fig. 15. Plots of: (a) distribution function $\varphi(\varepsilon; t)$ against adsorption energy values ε, (b) distribution function $\varphi(\varepsilon; t)$ as a function of time, and (c) the lateral molecular interaction energy $\beta\theta_i$ (dimensionless) as a function of time for C_2H_2, on CaO at 323.2 K. From Ref. [113] with permission.

while pressure gradient along the bed is negligible; (4) it leads directly to experimental isotherm without specifying an isotherm equation a priori; (5) the isotherm can be determined in the presence of a surface reaction of the adsorbate.

Regarding the stopped flow technique the RF-GC one surpasses as it does not need the continuously switching from a flow dynamic to a static system and vice versa, by repeatedly closing and opening the carrier gas flow.

Moreover, RF-GC does not depend on retention times, broadening factors, and statistical moments of the elution bands, due mainly to non-linear isotherms, non-negligible axial diffusion in the column, non-instantaneous equilibration between the mobile and the stationery phase, non-sharp input distribution of the analyte. Also, the results of RF-GC do not need extrapolation to infinite dilution and zero carrier gas flow-rate to approximate true physicochemical parameters.

Beyond that, it creates a domain of time-resolved chemistry for surfaces, which provides experimental local values of adsorption energies, adsorption isotherms, monolayer capacities, probability density functions and lateral molecular interactions. Thus, all physicochemical quantities mentioned above can be determined as functions of experimental time by means of a simple personal computer program, the LAT one [112,113] and the plots can be provided through a suitable software (e.g. Excel).

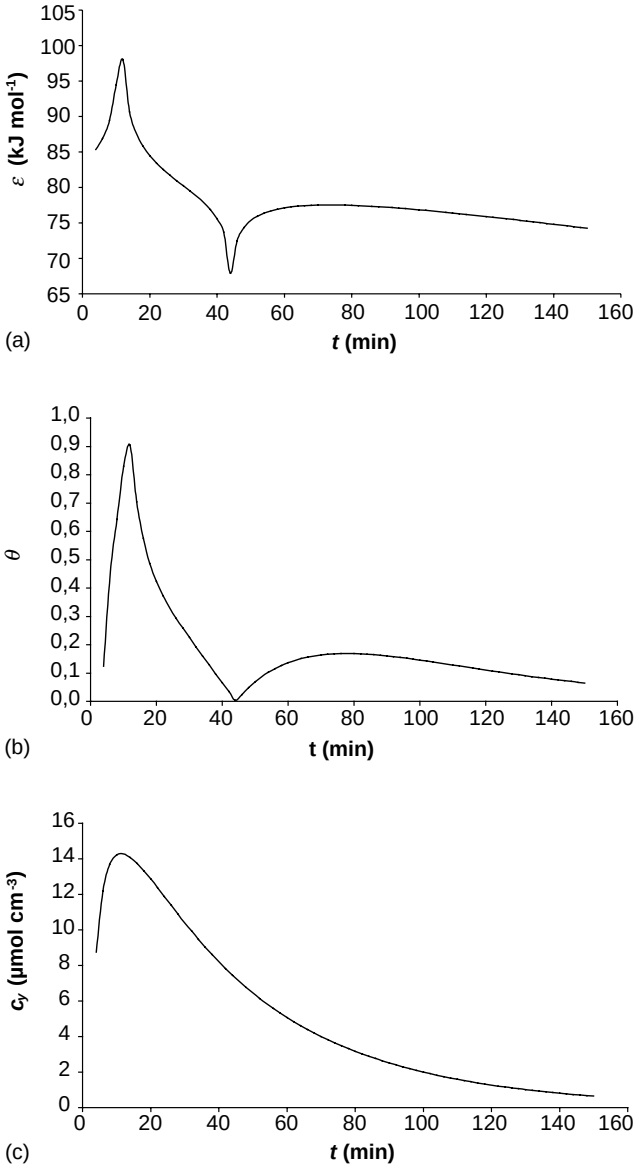

Fig. 16. Plots of: (a) local adsorption energy ε, (b) local adsorption isotherm θ_i and (c) gaseous adsorbate concentration c_y as a function of time for C_2H_2 on CaO at 323.2 K. From Ref. [113] with permission.

7. Characterization of materials through adsorption isotherms

Gas adsorption has for a long time been a standard technique to study solid adsorbents and to characterize surfaces with respect to their area and porosity. Some remarkable reviews by Poole and co-workers [129] and Eiceman et al. [130] and a book by Poole and Schuette [131] should be useful with a growing trend in stationary phase offerings. Discussion of methods to characterize the chromatographic properties of stationary phases can be found in the above mentioned review [129]. Thus, inverse gas chromatography (IGC) is a prominent method for exploring surface structure and interactions between solid surfaces and probe solutes. The main scope is the description and characterization of new and modified materials. Another interesting field is the study of synthetic adsorbents by the IGC. Thus, IGC was utilized to explore properties of several materials [130]. Special reports [132–138] have been included among others in this contemporary review. In addition, a new book by Poole [139] presents a comprehensive survey of modern chromatography. In general, the book is an excellent source of information on all aspects of chromatography. Several new topics have also been presented.

The discussion in this section focuses on reports where solid adsorbents are described or characterized with emphasis on new or modified materials. The more contemporary and representative applications will have been presented.

The concept of Integral Adsorption Equation has been widely used since its introduction by Ross and Olivier [15]. Given a local model, which expresses the adsorbed mass as a function of temperature and pressure on an energetically homogeneous surface, it is possible to calculate the corresponding adsorbed mass on a heterogeneous surface.

$$m(T, P) = \int_{\varepsilon_i}^{\varepsilon_f} m(T, P, \varepsilon) F(\varepsilon)\, \mathrm{d}\varepsilon \tag{46}$$

where m is the adsorbed local mass, T and P the corresponding temperature and pressure, ε the adsorption energy and $F(\varepsilon)$ the energy distribution function for a given adsorbate–adsorbent system.

Such a procedure has been applied to well known adsorption local models and for simple mathematical expressions of the energy distribution function. The analytical form of $F(\varepsilon)$ is assumed a priori. The parameters of the energy distribution function are determined by minimization of the discrepancies between experimental and calculated isotherms. Eq. (46), being solved by analytical or numerical way depending on the mathematical expressions chosen for $F(\varepsilon)$ and m_{local}. It is sometimes possible to determine analytically $F(\varepsilon)$ without assumption on its analytical expression using a given form for $m(T, P)$ and a simple local model. For example, the Freundlich, Dubinin–Radushkevich and Temkin empirical overall isotherm equations can be related to the Langmuir local model using respectively a decreasing exponential, a Gaussian and a constant energy distribution function [140].

Some authors [141–144] have tried to correlate the energy distribution function which is characteristic of the binary system adsorbate–adsorbent to the pore volume distribution function. This correlation can be easily established for activated carbons. Indeed, it is commonly assumed that activated carbons exhibit an energetically homogeneous surface. Their apparent heterogeneity on the energetic point of view is linked to their heterogeneous geometric structure. The integral adsorption equation concept coupled to an efficient modelling of the correlation between the energy distribution function and the pore volume distribution function allow the determination of the pore volume distribution function of such solids from adsorption experimental data.

The main advantage of such a function compared to the energy distribution function is that it can be considered as a characteristic of the adsorbent itself.

The availability of such functions is very interesting. Indeed, the adsorptive properties of activated carbons are widely governed by their porous structure, which is not the case for other sorbents like silica gels for which the adsorptive properties are mainly due to their surface heterogeneity. Different approaches have been used for the determination of the pore volume distribution function of activated carbons. Huber et al. [145], Dubinin [146], Jaroniec and Pietrowsha [147] have extended the basic Dubinin–Radushkevich equation considering it as a local model in Eq. (46). They have introduced a pore volume distribution function of the characteristic energy, which has a physical meaning similar to the adsorption energy. The characteristic energy has been related to the pore size of activated carbons [148] so that it is possible to replace the pore volume distribution function of this characteristic energy by the corresponding pore volume distribution of the pore size. This procedure is rather simple. It allows the determination of a pore volume distribution function, which should be independent of the adsorbate. Thus, it should be possible to simulate adsorption isotherms of a given adsorbate on a given carbon, using the pore volume distribution function of this adsorbent predetermined from adsorption data relevant to another adsorbate.

A third approach consists in using classical models such as the Langmuir, Volmer, Fowler–Guggenheim and Hill-de Boer models as local theory in Eq. (46) [144,149–151].

Frere et al. [140] have proposed a method for the determination of the micropore volume distribution function of activated carbons. This method is based on the integral adsorption equation. The micropore volume distribution function is assumed to be a Gaussian of which the parameters are unknown. These parameters are determined using adsorption isotherms of carbon dioxide on a given activated carbon. Several local adsorption models are used (Langmuir, Volmer, Fowler–Guggenheim, Hill-de Boer).

Among the numerous materials applied in adsorption, synthetic carbon adsorbents are of the most interest for their unique characteristics such as high thermal stability and chemical inertness as well as regulated porosity and surface chemistry [152,153]. Synthetic carbon adsorbents are characterized by a high degree of purity, high thermal stability under inert atmosphere conditions and electrical conductivity, hardness and resistance to corrosion. Because of these properties they find many applications. For its application in adsorption or in chromatography, adsorbent materials should have suitable sorption properties, and this concerns not only the sorption capacity, but also the texture of the carbonized material. Unique properties of carbon obtained by carbonization of polymers permit utilize these materials for special purposes, for which they are practically indispensable. For example Gierak and Seredych [154] have described the method of carbonization of organic polymers and utilization of so obtained synthetic spherical carbon adsorbents to blood hemoperfusion, i.e. sorption of toxins directly from patient's blood.

Gierak and Seredych [154] have reviewed the methods of preparation and modification the surface properties of synthetic carbon adsorbents, obtained by carbonization of different porous organic polymers. They paid special attention to applications of these adsorbents to trace analysis of organic pollutants in environmental samples. Thus, the physicochemical properties of synthetic carbon adsorbents are superior compared to those of the "traditional" active carbon materials.

From this point of view and for that reason the contribution of Katsanos and Roubani-Kalantzopoulou [155], Presented at the 4th International Symposium on the Effects of Surface Heterogeneity in Adsorption and Catalysis on Solids, in Poland, under the title "Time separation of surface heterogeneity through experimental measurement of adsorption energies, local monolayer capacities, local isotherms and energy distribution functions by inverse gas chromatography", seems to be an interesting one. All physicochemical quantities mentioned above can be determined as functions of experimental time. This creates a domain of time-resolved chemistry of surface, used to reach important conclusions regarding adsorption sites useful for characterization of new synthetic adsorbents.

Another interesting work is that from Terzyk et al. [156], where different methods of the calculation of fractal dimension of adsorbents are shortly reviewed. Freshly projected algorithms are applied to calculate D for two systems previously studied by Rudzinski et al., and the results are compared. Further a modification of the recently derived fractal analogue of the Dubinin–Astakhov adsorption isotherm equation was proposed to take into account the effect of multilayer adsorption. In [157], an attempt for estimation of micropore size distribution function from adsorption isotherm of nitrogen and benzene has been done. According to the "patch-wise" model of surface topography the experimental (global and not local as in [155]) adsorption isotherm represents an average over all values of the pore dimension/adsorption energies existing on the gas–solid interface. Such formulation of the problem leads again to the linear Fredholm equation of the first kind.

Although the introduction of porous polymers in gas–solid chromatography has provided a solution to many analytical problems, there remains considerable interest in inorganic adsorbents. Among adsorbents, silica gel has been one of the most thoroughly researched and characterized materials, since it offers surface properties covering a wide range of acidity, surface reactivity and pore structure. Thus, in an investigation of Faramawy et al. [158], various surface modified silica gels have been evaluated as stationary phase in gas chromatography with special emphasis on the role of surface reactivity and pore structure.

Solid surfaces of practical interest are energetically heterogeneous. Silicoborate glasses are not an exception. Such

glasses are extensively used in many material fields as fibres in reinforcing plastics, adsorbents, in chromatography, electronics, etc. In all these uses their surface energy and, more exactly, the distribution of active sites on the glass surface, plays an important role. Among other techniques, gas–solid adsorption is generally recognized as the most important for studying the energetic heterogeneity of solid surfaces [69,159–162]. Thus, Rubio et al. have studied the adsorption isotherms of methanol on four sodium silicoborate glasses as well as the adsorption isotherms of methanol, *n*-hexane, benzene and *n*-butylamine on SBI glass [69]. These results are quite similar to those obtained by Hsu et al. [75] and Jagiello et al. [163]. In all cases the laboratory prepared sodium silicoborate glasses slowed the same behavior and in most cases the commercial E-glass did not fit the results. This led us to the conclusion that the constituents of the E-glass other than SiO_2 or B_2O_3 (such as CaO, Al_2O_3) create another kind of heterogeneity on the glass surface.

Bakaeva et al. [70], have studied the heterogeneity of the glass fiber surface from inverse gas chromatography. The authors referred to some previous works emphasize that the calculation of the site energy distribution from adsorption IGC data is certainly not new, as it is reviewed many times, i.e. by Katsanos et al. [114], as well as in Rudzinski and Everett [11], Jaroniec [164] and Papirer and Balard [165]. The new in their work is that they obtain not only the energy but also the entropy distribution and the entropy/energy relationship for sites.

Since polyaromatic hydrocarbons and polychlorinated compounds are important pollutants in soil, Erhey et al. [166] have determined the adsorption isotherms for naphtalene, phenanthrene, hexachlorobenzene, and pentaclorophenol as model compounds on soil using an experimental technique based on frontal analysis chromatography.

In another work [167] the effects of concentration and temperature of 23 volatile organic compounds on Carbotrap B have been determined using frontal chromatography. Thus, original isotherms have been produced and adsorption parameters based on the Langmuir, Freundlich, and Dubinin–Polyani adsorption models have been calculated. It is only recently that effects of chronic exposure to ambient atmospheric levels of these compounds have been taken into consideration. Recently, Hsiech and Chen [168] proposed an adsorption isotherm model for two types of volatile organic compounds on a heterogeneous carbon surface. The Langmuir isotherm was used as a local isotherm for describing heterogeneous surfaces to obtain the adsorption energy distribution.

Inverse gas chromatography has been used by Inel et al. [169] to evaluate the adsorption parameters (ΔH, ΔS, ΔG) of some probes, each representing a class of organics (*n*-hexane, cycloexane and benzene) on zeolites as well as to construct the adsorption isotherms. A brief review of the different methods used to calculate the adsorption parameters in finite concentration and infinite dilution regions was included.

Phenol adsorption on carbonaceous materials, particularly activated porous carbons, is currently studied with respect to water pollution and the removal of phenol and its derivatives by adsorption. Thus, phenol physisorption on a series of porous and non-porous amorphous carbons was studied by Bertoncini et al. [170]. The simulated adsorption isotherms were compared with experimental results. Other characteristics published are adsorption energy distribution functions, distribution of molecules according to gas–solid energy, and local isotherms.

Evaluation of adsorption properties of low surface area and comparison of experiments with a theoretical study have been published by Kluson and Scaife [171]. More precisely, adsorption isotherms of nitrogen, argon and methane were experimentally measured on low surface area graphitized carbons and natural graphite.

Ribeiro Carrott et al. [172] have studied the adsorption of nitrogen, neopentane, *n*-hexane, benzene and methanol for the evaluation of pore sizes in silica grades of MCM-41. The adsorption isotherms of all these systems have been determined.

A somehow different application is that concerning the modeling of flavor release using inverse gas chromatography–mass spectrometry [173].

On the other hand, protein interactions with solid surfaces can affect the performance of many materials and processes, in areas ranging from medicine to biochemical engineering. Particuraly, adsorption of proteins on microspheres (monodisperse latex particles) is of great interest for biochemical applications. Thus, Baptista et al. [174], concluded that protein adsorption onto solid surfaces is controlled by the properties of the support surface, the nature of protein molecule and the solution conditions.

One of rapidly developing fields of materials chemistry is synthesis, characterization and application of nanoporous solids. These materials exhibit remarkable structural and surface properties, which make them suitable as adsorbents, chromatographic packings, catalysts and catalyst supports. A proper characterization of porosity and surface properties plays a key role in synthesis and application. Gas adsorption appears to be the most suitable characterization method, since it allows information to be obtained about both pore size distribution and surface characteristics of the materials. From this point of view, Kruk et al. [175] have published a comparative analysis of simple and advanced sorption methods for assessment of microporosity.

From another point of view a basic study of the submonolayer physical adsorption through local isotherms has been published recently by Steele and Bottani [176,177]. Simulations of the adsorption of nitrogen on several model heterogeneous surfaces are analyzed using an alternative description in which the surface is treated as a collection of supersites, each of which can hold 5–6 molecules in the complete monolayer. The local isotherm that is used to describe the sub-monolayer adsorption on a supersite is taken to be the truncated virial isotherm. The advantages

and disadvantages of this approach are discussed and it is concluded that the supersite concept is a promising approach to the description of adsorption on realistic models of heterogeneous surfaces.

A key ingredient in the analysis of an adsorption process is the accurate and thermodynamically consistent description of the equilibrium behavior of the system. Apart from providing the limiting amount that can be adsorbed at given conditions, the isotherm or model of the gas–solid equilibrium is important to the analysis of transport processes in the adsorbent and the associated uptake dynamics. Consequently considerable attention has been devoted in the literature to the development of isotherm models for single and multicomponent systems. Ding and Bhatia [178] have re-formulated the vacancy theory of adsorption through the mass-action law, and placed a convenient framework permitting the development of thermodynamically consistent isotherms.

8. Characterization of materials through kinetic quantities based on experimental adsorption isotherms

The RF-GC method offers many possibilities for physicochemical measurements, as rate and distribution constants, experimental isotherms, deposition velocities and reaction probabilities, mass transfer coefficients, all pertaining to the mechanism of homogeneous and/or heterogeneous reactions.

In this section, some cases studies referring to the physicochemical behavior and characterization of some important materials under different atmospheric conditions have been collected:

8.1. Case study 1

The surface-coating industry is indeed an ancient one. The origin of paints dates back to prehistoric times. It has been in more recent years, however, that the surface-coating industry has made its greatest strides, which can be attributed to the results of scientific research and the application of modern engineering. Pigments are coloured, organic and inorganic insoluble substances, which are used widely in surface coatings. White lead, zinc oxide and zinc chromate (lithopone) were once the principal white pigments. Today titanium oxide in many varieties is almost the only white pigment used. Coloured pigments consisted among others of lead chromate, and cadmium sulfide. Both of them are yellow [91].

The industrialized society of the 20th Century, as it is known, has caused a radical change in the conditions of preservation and conservation of monuments, buildings and metallic structures, and the atmospheric pollution associated with industrialization is currently threatening extinction for both cultural heritage and nature itself. General industrial emissions come mainly from evaporation during the storage, transportation and utilization of organic chemicals. Whilst emissions occur from a variety of industries, the petroleum industry is the main industrial source of troposphere volatile hydrocarbons.

The more reactive hydrocarbons are expected to perform a key role in the formation of secondary pollutants in urban areas close to emissions sources. What is really important is the kinetic study of interaction of these hydrocarbons with pigments, which consists the coloured basis of different paints of works of art. On the other hand, it is known that any heterogeneous reaction between a solid and a gas consists of the following four basic steps:

(1) Mass tranfer of the gas reactant to the gross exterior surface of the solid material.
(2) Diffusional transfer of the gas in and out of the pores of the solid.
(3) Adsorption (rather activated) of the gas at the interface.
(4) Possible surface chemical reaction of the adsorbed reactant.

Steps 1–3 can be simplified by considering two overal mass transfer coefficients, one in the gas phase and one in the solid phase. It is their ratio that gives the equilibrium constant for the distribution of the gas between the solid and gaseous phases, according to the linear isotherm model. But as mentioned elsewhere, the linear model is inexact when treating with inorganic oxides and sulfides. For this inadequacy the non-uniformity of the surface sites is above all the more responsible. For that reason the linear model is abandoned and replaced by the directly measured experimental isotherm.

Reversed-flow gas chromatography was used to study the kinetics of the action of five hydrocarbons namely, ethane, ethene, ethyne, propene and butene and of the nitrogen dioxide, on three known and widely used pigments, the white one TiO_2, and the yellows CdS and $PbCrO_4$ [91].

The calculation of kinetic parameters and mass transfer coefficients is based on an experimental adsorption isotherm. All these calculations are based on a non linear adsorption isotherm model as it is well accepted that the linear one is inadequate for inorganic substances like these mentioned in this work. The inadequacy is mainly attributed to the non-uniformity of the solid surface. Five physicochemical parameters have been obtained for each of the twenty heterogeneous reactions studied. With these systematic experiments under conditions which are similar to the atmospheric ones, an extrapolation of the results obtained to ≪real≫ atmospheres with a high degree of confidence is possible. Some of the calculations were based on the linear model for comparison.In the present work a physicochemical study of the reactions between each of the three pigments and the six gases is carried out, according to the non-linear model, with this new chromatographic technique known as RF-GC. Some of the calculations were based on the linear model for comparison.

From all these physicochemical quantities measured under the same experimental conditions, it is obvious a much more different behavior of the three pigments as well as

of the six gaseous reactants. This is justified by the different chemical compositions of them. Among the solids, TiO_2 seems to be the most reactive and CdS the less. Among the hydrocarbons, the unsaturated ones are more reactive than the saturated ethane, and the hydrocarbons with the lower molecular weight exhibit the highest reactivity. Nitrogen dioxide on the other hand has a significant attack by itself and it is possible by means of RF-GC technique to measure precisely its recognized attack.

Thus, by means of the constants k_1, k_{-1} the reversible phenomena of adsorption–desorption, taking place in the gas–solid boundaries, are studied in a quantitative level (order of magnitude 10^{-3}), while through the k_2 (order of magnitude 10^{-5}), any irreversible phenomenon can be investigated.

Contrarily to other techniques, either chromatographic or not, which take the adsorption phenomena as negligible, all k_{-1} values provided by this one lead to more realistic models and mechanisms. Moreover, the mass transfer coefficients related directly to the adsorption–desorption phenomena provide a steady scientific basis for kinetic data interpretation.

Finally, the experimental data concerning diffusion coefficients, rate constants etc are in good agreement with the results obtained by other scientific groups with the same or other techniques.

8.2. Case study 2

The RF-GC method is a powerful tool for the investigation and study of all corrosion phenomena through some simple chromatographic experiments. Lately this method has been successfully applied to the study of the impact of air pollutants, organic and/or inorganic, on many solids such as marbles, stones, etc. The present work [95], focuses on the determination of kinetic quantities for about 30 heterogeneous reactions including three known pigments, two oxides and one sulfide, and five light hydrocarbons which exist in the atmosphere in great quantities, in the presence or not of the corrossive pollutant NO_2. All measurements were based on the real experimental adsorption isotherms, not necessarily linear, which admittedly are the only correct ones for such studies. This type of isotherms is very rare in the literature.

Deposition velocities, V_d, reaction probabilities, γ and local adsorption parameters, k_1, describing the isotherms of ethane, ethene, ethyne, propene and 1-butene onto three solid pigments (PbO, Fe_2O_3, CdS) have been determined in the absence and in the presence of NO_2, together with the surface reaction rate constant, k_2, and the desorption rate constant, k_{-1}. The calculations are based on experimental adsorption isotherms, since the linear adsorption model is not a very good approximation for inorganic solids, like those mentioned above. The importarnt result found is the effect of NO_2 on the values of the parameters V_d, γ, k_1, k_{-1} and k_2 in most cases.

The catalytic effects of the nitrogen dioxide on the reactions between the various hydrocarbons studied and some of the pigments used are demonstrated by the higher values of the experimentally obtained deposition velocities and reaction probabilities in most cases. Among the various kinds of the hydrocarbons studied with the RF-GC technique, some of them appear more reactive than the others. Obviously, to explain the influence of NO_2 on the various physicochemical parameters, one needs some knowledge about the detailed mechanism of the phenomena, which almost certainly include blocking of adsorption active sites by NO_2 molecules or creation of new ones by it. The kinetic model that describes these gas–solid interactions may be the following.

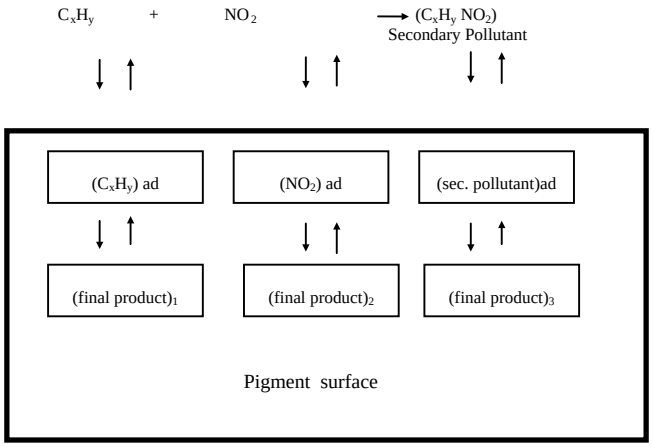

Fig. 17. Possible homogeneous and heterogeneous interactions among pollutants and pigment surface. From Ref. [95] with permission.

When the pollutants reach the pigment surface, an adsorption process is possible leading to the adsorbed species and followed by the final products of the heterogeneous reactions. The product of the possible homogeneous reaction may have the same behaviour. All these interactions may be reversible (cf. Fig. 17).

What, in reality, will have a senior significance in the future is the identification of all these intermediates and final products mentioned, by the appropriate techniques. But the present work enables us to investigate whether a synergy exist between these pollutants and solids and that is achieved through the calculation of the six fundamental physicochemical quantities pertaining to any of the 30 heterogeneous reactions. These values constitute a wealth of information showing what a simple gas chromatographic arrangement can offer to surface and atmospheric chemists and chemical engineers, instead of the conventional global rate constants.

Hence, the most important result is that the experimentally observed values of deposition velocity, V_d, and reaction probability γ are influenced by the presence of nitrogen dioxide. Probably, the synergistic effects between hydrocarbons and nitrogen dioxide lead to much greater damage and corrosion of these pigments in some cases, and perhaps of many others. As these pigments have been widely used as paints for many works of art, the significance of these results is obvious. Thus the coexistance of light hydrocarbons with nitrogen dioxide on the pigments' surface has a great economic and social impact.

8.3. Case study 3

The anthropogenic sources of pollutants include combustion and evaporation of fuels, as well as evaporation of solvents. Exhaust gases are the major sources of hydrocarbon emissions in urban areas. Aromatic hydrocarbons represent a significant constituent of many fuels (e.g. gasoline), as well as of automobile exhausts. Benzene (2470 ppb) and toluene (3830 ppb) are the most abundant aromatic volatile hydrocarbons. Diurnal variations of these hydrocarbons show that the highest concentrations are measured during the early morning and late afternoon and the similarity of the profiles suggests that the motor exhaust emissions are the dominant source of aromatic hydrocarbons [93].

Once released into the atmosphere, these pollutants, as well as other organic and inorganic ones, may undergo a variety of complex interactions through physical, chemical and photochemical processes occurring during their residence time.

The interaction of materials with the atmosphere has received increased attention. Moreover historical buildings and monuments, especially in Europe, are decorated with works of art, on their exterior surfaces suffering not only time and weather injuries but the fateful attack of air pollution too. As for the different works of art, there is no mechanism of self-protection and regeneration for the materials used in artistic objects, e.g. pigments as these studied here. For instance, an important phenomenon taking place on monuments' surfaces is the so called pile-up, i.e. the deposition of exogenous chemical compounds. Unfortunately, measurements of the deposition rate are not easy. Another important question arises from the presence of secondary pollutants produced by chemical reactions between primary pollutants. All the above show how complicated the problem is. Given all these difficulties, it seems that the evaluation of many physicochemical parameters and the determination of the correlation between pollutant concentration and damage through a mechanism constitute the first step for artistic heritage conservation. The interaction of benzene and toluene on five known pigments, namely ZnO, PbO, Fe_2O_3, Cr_2O_3, and TiO_2 has been studied, in the presence as well as in the absence of nitrogen dioxide [93]. The following physicochemical constants have been determined and therefore the materials' behavior in such a polluted atmosphere is concluded: (1) the dynamic adsorption rate constant of the analyte pollutant, describing its experimental isotherm on the surface of the material varying with the time, (2) the desorption rate constant of the pollutant from the solid surface, (3) the rate constant of a possible surface reaction of the adsorbed analyte (first or pseudo-first-order), (4) the overall deposition velocity of the pollutant, (5) the reaction probability of the pollutant on the material and (6) the apparent rate constant of a possible chemical reaction of each aromatic pollutant with nitrogen dioxide, taking place above the material and simultaneously with the heterogeneous one. The contribution of the above parameters to the elucidation of the mechanism of deterioration of various works of art in museums is significant, as one can see. The five pigments display a different behavior in the same polluted atmosphere.

With regard to the deposition velocity values, one can write the following relations:

(i) In the case of benzene:

$$V_{d,PbO} \gg V_{d,ZnO} \cong V_{d,Fe_2O_3} > V_{d,TiO_2} \gg V_{d,Cr_2O_3}$$

(ii) In the case of toluene:

$$V_{d,PbO} \gg V_{d,TiO_2} > V_{d,Fe_2O_3} > V_{d,ZnO} \gg V_{d,Cr_2O_3}$$

In the presence of nitrogen dioxide, the above relations are modified respectively to:

(i) $V_{d,PbO} \gg V_{d,TiO_2} > V_{d,ZnO} > V_{d,Fe_2O_3} \gg V_{d,Cr_2O_3}$
(ii) $V_{d,PbO} \gg V_{d,TiO_2} \gg V_{d,Fe_2O_3} > V_{d,ZnO} \gg V_{d,Cr_2O_3}$

That is, except for C_6H_6–ZnO and C_6H_6–TiO_2, no other change has taken place.

For the reaction probability values, the relations are:

(i) In the case of benzene:

$$\gamma_{PbO} \gg \gamma_{ZnO} \cong \gamma_{Fe_2O_3} > \gamma_{TiO_2} > \gamma_{Cr_2O_3}$$

(ii) In the case of toluene:

$$\gamma_{PbO} \gg \gamma_{TiO_2} > \gamma_{Fe_2O_3} > \gamma_{ZnO} \gg \gamma_{Cr_2O_3}$$

In the presence of nitrogen dioxide, the following are extracted, respectively:

(i) $\gamma_{PbO} \gg \gamma_{TiO_2} > \gamma_{ZnO} > \gamma_{Fe_2O_3} \gg \gamma_{Cr_2O_3}$
(ii) $\gamma_{PbO} >> \gamma_{TiO_2} >> \gamma_{Fe_2O_3} > \gamma_{ZnO} >> \gamma_{Cr_2O_3}$

One can observe that the two physicochemical quantities V_d and γ change in the same way as far as the same heterogeneous system is concerned.

Moreover, from all these values, one can rigorously conclude that a synergistic effect takes place in four systems:

$C_6H_5CH_3$–NO_2–PbO
$C_6H_5CH_3$–NO_2–TiO_2
C_6H_6–NO_2–PbO
C_6H_6–NO_2–TiO_2

while, in the remaining cases, the presence of the inorganic pollutant seems to minimize the attack.

With respect to the rate constant k_2 we observe a real increase of this quantity in the next cases:

$C_6H_5CH_3$–NO_2–ZnO
$C_6H_5CH_3$–NO_2–PbO (the highest)
C_6H_6–NO_2–Fe_2O_3
C_6H_6–NO_2–TiO_2

and a clear decrease in the following systems:

$C_6H_5CH_3$–NO_2– Fe_2O_3
$C_6H_5CH_3$–NO_2–Cr_2O_3
C_6H_6–NO_2– Cr_2O_3
C_6H_6–NO_2–PbO

Finally, the apparent rate constants of the homogeneous reactions are of the same magnitude of order, with a mean value of $2.60 \times 10^{-4}\ s^{-1}$ for C_6H_6–NO_2 and $1.75 \times 10^{-4}\ s^{-1}$ for $C_6H_5CH_3$–NO_2.

8.4. Case study 4

Ozone plays a significant role in the atmospheric chemistry. Its importance in the troposphere as well as in the stratosphere is particularly well documented [84]. Among the various classes of compounds present in the troposphere, unsaturated hydrocarbons are unique in exhibiting significant reactivity towards ozone, hydroxyl, and nitrate radicals. A major role of the ozone–alkene reaction has been recognized since these reactions can provide mutual sinks for both ozone and alkenes and serve as sources of partially oxidized compounds, e.g. CO, aldehydes, ketones and organic acids. Our present knowledge of the chemical and physical processes that govern such a reaction, e.g. aerosol formation in the atmosphere, is still rather limited and further studies are needed in most of the relevant areas of research.

In this work [84], the diffusion coefficients of ethene and ethyne in a mixture of nitrogen and ozone had been determined by the RF-GC method. The next stage was the kinetic study of homogeneous systems C_2H_2–O_3 and C_2H_4–O_3. Finally the initial (Rk_1) and the final (V_d) deposition velocities, the desorption rate constant (k_{-1}) the reaction probability as well as the first order rate constant (k_2) for possible surface reaction have been determined for the heterogeneous systems C_2H_2–O_3–γ-Al_2O_3, C_2H_4–O_3–γ-Al_2O_3, C_2H_2–γ-Al_2O_3, C_2H_4–γ-Al_2O_3.

Thus, using simple chromatographic arrangements which are simulating a simple model for the action of different gases on solids in the laboratory scale (cf. Fig. 17), three rate constants (k_1, k_{-1}, k_2), as well as the initial (Rk_1) and the final (V_d) deposition velocities and the wall reaction probability (γ), have been determined. Through those parameters, which constitute a wealth of information, a chemist or a chemical engineer can extract valuable results about the detailed mechanism of these heterogeneous reactions. Moreover, using this technique, it is also possible to study a homogeneous reaction, like those between O_3 and C_2H_2 or C_2H_4, in order to draw safer kinetic results. Finally, it is possible to study by the same technique simultaneously two reactions, one homogeneous and the other heterogeneous. In every case, the RF-GC technique combined with the denuder devices, provides a valuable tool in a modern physical chemistry laboratory.

8.5. Case study 5

Hydrogen is chemisorbed dissociatively on ZnO, and the surface species have been identified by their infrared spectra [179]. One hydrogen atom becomes bonded, as a proton, to a surface oxygen atom (identified by the O–H stretching frequency) and the other becomes bonded to an exposed zinc atom, as a hydride ligand (identified by the Zn–H stretching frequency).

Adsorption of propene on the surface of ZnO may be expected analogous to the ethene adsorption which is rapid and reversible. Evidently the ethene is chemisorbed, and some may be physisorbed as well. The simplest model of linear adsorption is sometimes a good approximation for adsorption on solids with nearly uniform surfaces, it usually fails to provide an accurate representation when the adsorbent is an inorganic solid of the kinds used as catalysts. In these cases a non-linear model is of great value. In contrast to the former, the latter is more precise as it accounts for the more realistic conditions of the experiment and therefore gives a much better representation of adsorption than the linear isotherm [180].

When hydrogen and propene are simultaneously present on the surface of ZnO, they are catalytically converted into propane. The chemistry is complicated at high temperatures, but at temperatures of about 100 °C, Kokes and Dent [181,182] found that the surface and catalytic chemistry are so simple that they could use infrared spectroscopy to investigate the catalyst in the working state and to elucidate many details of the catalysis.

The application, of the RF-GC as a technique for measuring physicochemical quantities, has been used in the past and also recently for analogous studies. In this work [179] it will be shown that a wealth of physicochemical quantities pertaining to heterogeneous catalysis can be determined simultaneously by using the above technique, which requires a very simple experimental set-up, and adopting a linear and a non-linear adsorption isotherm. With a gas chromatography apparatus, a series of experiments was carried out, permitting the calculation of fundamental physicochemical quantities pertaining to heterogeneous catalysis. Thus, many physicochemical constants for the propene hydrogenation reaction catalysed on zinc oxide, have been determined using a linear and a non-linear adsorption isotherm by the RF-GC. These are adsorption–desorption rate constants, surface reaction rate constants, adsorption equilibrium constants for propene, overall mass transfer coefficients in the gas phase and in the solid catalyst across the phase boundary, deposition velocities and reaction probabilities of the hydrocarbon onto zinc oxide. The above parameters were determined at various termperatures of the catalytic bed for the hydrogenation of propene. The results obtained can help to understand the mechanism of reactions on solid semiconductor catalyst surfaces such as ZnO, and confirm experimentally the theoretical calculations in adsorption and heterogeneous catalysis.

Acknowledgements

Support of this work by the European Union with the contract EV5V-CT94-0537,as well as by the Technical University of Athens with the contract 65/1181/2002 is gratefully acknowledged.

References

[1] J.A.V. Butler, Proc. R. Soc. A 135 (1932) 348.
[2] E.A. Guggenheim, Modern Thermodynamics, Methuen, London, 1933 (Chapter XII).
[3] T.L. Hill, J. Chem. Phys. 17 (1949) 507, 520.
[4] T.L. Hill, J. Chem. Phys. 18 (1950) 246.
[5] D.H. Everett, Trans Faraday Soc. 46 (1950) 453, 942, 957.
[6] A.I. Rusanov, Phase Equilibria and Surface Phenomena, Khimia, Leningrad, 1967.
[7] D.S. Jovanovic, Koll. Z. Z. Polym. 235 (1969) 1203, 1214.
[8] D.H. Everett, Thermochemie, in: Proceedings of the International Coll. CNRS, Paris, vol. 201, 1972, p. 45.
[9] W.A. Steele, The Interaction of Gases with Solid Surfaces, Pergamon, Oxford, 1974.
[10] W. Rudzinski, S. Sokolowski, Surf. Sci. 65 (1977) 593.
[11] W. Rudzinski, D.H. Everett, Adsorption of Gases on Heterogeneous Surfases, Academic Press, New York, London, 1992 (Chapter 1).
[12] C. Domb, Adv. Phys. 9 (1960) 149.
[13] A. Clark, The Theory of Adsorption and Catalysis, Academic Press, New York, London, 1970 (Chapter 1).
[14] A.F. Devonshire, Proc. R. Soc. London A 163 (1937) 132.
[15] S. Ross, J.P. Olivier, On Physical Adsorption, Wiley/Interscience, New York, 1964.
[16] T.L. Hill, J. Chem. Phys. 17 (1949) 762.
[17] B. Charmas, R. Leboda, J. Chromatogr. A 886 (2000) 133.
[18] J.A. Morrisson, J.M. Los, L.E. Drain, Trans. Faraday Soc. 47 (1951) 1023.
[19] L.E. Drain, J.A. Morrisson, Trans. Faraday Soc. 48 (1952) 840.
[20] L.E. Drain, J.A. Morrisson, Trans. Faraday Soc. 49 (1953) 654.
[21] J.D. Morrisson, S. Ross, Surf. Sci. 39 (1973) 21.
[22] S. Ross, J.D. Morrisson, Surf. Sci. 52 (1975) 103.
[23] A.W. Adamson, I. Ling, Adv. Chem. 33 (1961) 51.
[24] C. Sanford, S. Ross, J. Phys. Chem. 58 (1954) 288.
[25] S. Ross, J.P. Olivier, J. Phys. Chem. 65 (1961) 608.
[26] P. Gauden, P. Kowalczyk, A.P. Terzyk, Langmuir 19 (2003) 4253.
[27] A.V. Morozov, Methods for Solving Incorrectly Posed Problems, Springer, Berlin, 1984.
[28] N.A. Tikhonov, Y.V. Arsenin, Solutions of Ill-Posed Problems, Winston & Sons, New York, 1997.
[29] W. Rudzinski, W.A. Steele, G. Zgrablich (Eds.), Equilibria and Dynamics of Gas Adsorption on Heterogeneous Solid Surfaces, Elsevier, Amsterdam, 1997.
[30] R. Wojsz, Characterization on the Structural and Energetic Heterogeneity of Microporous Carbon Adsorbents Regarding the Adsorption of Polar Substances UMK, Torun, 1989.
[31] H. Jankowska, A. Swiotkowski, J. Choma, Active Carbon, Ellis Horwood, New York, 1991.
[32] D.D. Do, Adsorption Analysis: Equilibria and Kinetics, Imperial College Press, London, 1998.
[33] S.J. Gregg, K.S.W. Sing, Adsorption Surface Area and Porosity, Academic Press, London, 1982.
[34] M.M. Dubinin, in: D.A. Cadenhead (Ed.), Progress in Membrane and Surface Science, vol. 9, Academic Press, New York, 1975, p. 1.
[35] C.F. Cerofolini, N. Re, Riv. Nuovo Cimento Soc. Ital. Fis. 16 (1993) 1.
[36] M. Jaroniec, R. Madey, Physical Adsorption on Heterogeneous Solids, Elsevier, Amsterdam, 1988.
[37] W.A. House, M. Jaycock, Coll. Polym. Sci. 256 (1978) 52.
[38] I.K. Koopal, C.H.W. Vos, Coll. Surf. A 14 (1985) 87.
[39] A.W. Adamson, Coll. Surf. A 118 (1996) 193.
[40] R.S. Sacher, I.D. Morrison, J. Coll. Interf. Sci. 70 (1979) 153.
[41] C.H.W. Vos, I.K. Koopal, J. Coll. Interf. Sci. 105 (1985) 183.
[42] P. Brauer, M. Fassier, M. Jaroniec, Thin Solid Films 123 (1985) 245.
[43] I.K. Koopal, C.H.W. Vos, Langmuir 9 (1993) 2593.
[44] J. Jagiello, Langmuir 10 (1994) 2778.
[45] M. Szombathely, M. Brauer, M. Jaroniec, J. Comput. Chem. 13 (1992) 17.
[46] V.Sh. Mamleev, E.A. Bekturov, Langmuir 12 (1996) 441.
[47] B.J. Stanley, S.E. Bialkowski, D.B. Marshall, Anal. Chem. 65 (1993) 259.
[48] S.W. Provencher, Comput. Phys. Commun. 27 (1982) 213.
[49] S.W. Provencher, Comput. Phys. Commun. 27 (1982) 229.
[50] S.W. Provencher, CONTIN Users Manual, Version 2: Max-Planck-Institut fur Biophysikalische Chemie, Göttingen, 1984.
[51] P.C. Hansen, Numer. Algorithms 6 (1994) 1.
[52] J.A. LumWan, L.R. White, J. Chem. Soc., Faraday Trans. 87 (1991) 3051.
[53] F. Vilieras, L.J. Michot, F. Bardot, J.M. Cases, M. Francois, W. Rudzinski, Langmuir 13 (1997) 1104.
[54] C. Nguyen, H.D. Do, Langmuir 16 (2000) 1319.
[55] H.D. Do, Langmuir 18 (2002) 93.
[56] H.D. Do, Coll. Surf. A 187–188 (2001) 51.
[57] C. Nguyen, D.D. Do, J. Phys. Chem. B 104 (2000) 11435.
[58] A.P. Terzyk, P.A. Gauden, P. Kowalczyk, Carbon 40 (2002) 2879.
[59] P. Kowalczyk, A.P. Terzyk, P.A. Gauden, R. Leboda, E. Szmechtig-Gauden, G. Rychlicki, Z. Ryu, H. Rong, Carbon 41 (2003) 1113.
[60] P. Kowalczyk, V.M. Gunco, A.P. Terzyk, P.A. Gauden, H. Rong, Z. Ryu, D.D. Do, Appl. Surf. Sci. 206 (2003) 67.
[61] P. Kowalczyk, A.P. Terzyk, P.A. Gauden, V.M. Gunco, J. Coll. Interf. Sci. 256 (2002) 378.
[62] A.V. Kiselev, Ya. I. Yashin, Gas Adsorption Chromatography, Plenum Press, New York, 1969.
[63] J.R. Conder, C.L. Young, Physicochemical Measurement by Gas Chromatography, Wiley, New York, 1979 (Chapter 9).
[64] R.G. Laub, R.L. Pecsok, Physico-chemical Applications of Gas Chromatography, Wiley, New York, 1978.
[65] F. Dondi, M.F. Gonnord, G. Guiochon, J. Coll. Interf. Sci. 62 (1977) 30362 (1977) 303.
[66] F. Dondi, M.F. Gonnord, G. Guiochon, J. Coll. Interf. Sci. 62 (1977) 316.
[67] B.J. Stanley, G. Guiochon, Langmuir 11 (1995) 1735.
[68] I. Quinones, G. Guiochon, J. Coll. Interf. Sci. 183 (1996) 57.
[69] F. Rubio, J. Rubio, J.L. Oteo, Coll. Surf. 139 (1998) 227.
[70] T.I. Bakaeva, C.G. Pantano, C.E. Loope, V.A. Bakaev, J. Phys. Chem. B 104 (2000) 8518.
[71] A. Waksmundzki, S. Sokolowski, J. Rayss, Z. Suprynowicz, M. Jaroniec, Sep. Sci. 11 (1976) 29.
[72] M. Jaroniec, R. Leboda, S. Sokolowski, A. Waksmundzki, Sep. Sci. 11 (1976) 411.
[73] S. Sokolowski, R. Leboda, A. Waksmundzki, Ann. Soc. Chim. Pol. 50 (1976) 1565, 1719.
[74] W. Rudzinski, A. Waksmundzki, R. Leboda, M. Jaroniec, Chromatographia 7 (1974) 663.
[75] C.C. Hsu, W. Rudzinski, W. Wojciechowski, Chromatographia 8 (1975) 663.
[76] A. Waksmundzki, M. Jaroniec, Z. Suprynowicz, J. Chromatogr. 110 (1975) 381.
[77] R. Leboda, S. Sokolowski, J. Rynkowski, T. Paryjczak, J. Chromatogr. 138 (1977) 309.
[78] R. Leboda, S. Sokolowski, J. Coll. Interf. Sci. 61 (1977) 365.
[79] E. Kalogirou, I. Bassiotis, Th. Artemiadi, S. Margariti, V. Siokos, F. Roubani-Kalantzopoulou, J. Chromatogr. A 969 (2002) 81.
[80] N.A. Katsanos, J. Chem. Soc., Faraday Trans. I 78 (1982) 1051.
[81] N.A. Katsanos, Flow Perturbation Gas Chromatography, Marcel Dekker, New York, Basel, 1988.
[82] E. Arvanitopoulou, N.A. Katsanos, E. Metaxa, F. Roubani-Kalantzopoulou, Atmos. Environ. 28 (1994) 2407.
[83] V. Sotiropoulou, G.P. Vasilev, N.A. Katsanos, H. Metaxa, F. Roubani-Kalantzopoulou, J. Chem. Soc., Faraday Trans. 91 (1995) 485.

[84] G. Karagiorgos, F. Roubani-Kalantzopoulou, Z. Phys. Chem. 203 (1998) 231.
[85] J. Roles, G. Guiochon, J. Chromatogr. 591 (1992) 233.
[86] N.A. Katsanos, F. Roubani-Kalantzopoulou, J. Chromatogr. A 710 (1995) 191.
[87] X. Yun, Z. Long, D. Kou, X. Lu, H. Li, J. Chromatogr. A 736 (1996) 151.
[88] B. Gates, Catalytic Chemistry, Wiley, New York, 1992, p. 326.
[89] F. Roubani-Kalantzopoulou, J. Chromatogr. A 806 (1998) 293.
[90] A. Kalantzopoulos, Ch. Abatzoglou, F. Roubani-Kalantzopoulou, Coll. Surf. A 151 (1999) 377.
[91] St. Birbatakou, I. Pagopoulou, A. Kalantzopoulos, F. Roubani-Kalantzopoulou, J. Chim. Phys. 95 (1998) 2180.
[92] H. Metaxa, E. Kalogirou, F. Roubani–Kalantzopoulou, Russian J. Phys. Chem. 73 (1999) 112.
[93] A. Kalantzopoulos, S. Birbatakou, F. Roubani-Kalantzopoulou, Atmos. Environ. 32 (1998) 1811.
[94] Ch. Abatzoglou, E. Iliopoulou, N.A. Katsanos, F. Roubani-Kalantzopoulou, A. Kalantzopoulos, J. Chromatogr. A 775 (1997) 211.
[95] H. Zahariou-Rakanta, A. Kalantzopoulos, F. Roubani-Kalantzopoulou, J. Chromatogr. A 776 (1997) 275.
[96] N.A. Katsanos, F. Roubani-Kalantzopoulou, J. Chromatogr. A 710 (1995) 191.
[97] K.R. Atta, D. Gavril, G. Karaiskakis, J. Chromatogr. Sci. 41 (2003) 123.
[98] V. Loukopoulos, D. Gavril, G. Karaiskakis, Instrum. Sci. Technol. 31 (2003) 165.
[99] J. Kapolos, N.A. Katsanos, J. Chromatogr. A 977 (2002) 107.
[100] D. Gavril, K.A. Rashid, G. Karaiskakis, J. Chromatogr. A 919 (2001) 349.
[101] K.R. Atta, D. Gavril, G. Karaiskakis, Instrum. Sci. Technol. 30 (2002) 67.
[102] D. Gavril, K.A. Rashid, G. Karaiskakis, J. Chromatogr. A 919 (2001) 349.
[103] K.A. Rashid, D. Gavril, N.A. Katsanos, G. Karaiskakis, J. Chromatogr. A 934 (2001) 31.
[104] D. Gavril, N.A. Katsanos, G. Karaiskakis, J. Chromatogr. A 852 (1999) 507.
[105] D. Gavril, G. Karaiskakis, J. Chromatogr. A 845 (1999) 67.
[106] D. Gavril, A. Koliadima, G. Karaiskakis, Langmuir 15 (1999) 3798.
[107] D. Gavril, A. Koliadima, G. Karaiskakis, Chromatographia 49 (1999) 285.
[108] N.A. Katsanos, N. Rakintzis, F. Roubani-Kalantzopoulou, E. Arvanitopoulou, A. Kalantzopoulos, J. Chromatogr. A 845 (1999) 103.
[109] N.A. Katsanos, E. Arvanitopoulou, F. Roubani-Kalantzopoulou, A. Kalantzopoulos, J. Phys. Chem. B 103 (1999) 1152.
[110] N.A. Katsanos, E. Iliopoulou, F. Roubani-Kalantzopoulou, E. Kalogirou, J. Phys. Chem. B 103 (1999) 10228.
[111] F. Roubani-Kalantzopoulou, Th. Artemiadi, I. Bassiotis, N.A. Katsanos, V. Plagianakos, Chromatographia 53 (2001) 315.
[112] N.A. Katsanos, F. Roubani-Kalantzopoulou, E. Iliopoulou, I. Bassiotis, V. Siokos, M.N. Vrahatis, V.P. Plagianakos, Coll. Surf. A 201 (2002) 173.
[113] S. Margariti, V. Siokos, F. Roubani-Kalantzopoulou, J. Chromatogr. A 1018 (2003) 213.
[114] N.A. Katsanos, R. Thede, F. Roubani-Kalantzopoulou, J. Chromatogr. A 795 (1998) 133.
[115] N.A. Katsanos, F. Roubani-Kalantzopoulou, Adv. Chromatogr. 40 (2000) 231.
[116] I. Topalova, A. Niotis, N.A. Katsanos, V. Sotiropoulou, Chromatographia 41 (1995) 227.
[117] M. Domingo-Garcia, F.J. Lopez-Garzon, R. Lopez-Garzon, C. Moreno-Castilla, J. Chromatogr. 324 (1985) 19.
[118] J. Jaroniec, Phys. Lett. 59A (1976) 259.
[119] J.F. Parcher, K.J. Hyver, J. Chromatogr. 302 (1984) 195.
[120] V. Sotiropoulou, N.A. Katsanos, H. Metaxa, F. Roubani-Kalantzopoulou, Chromatographia 42 (1996) 441.
[121] F. Roubani-Kalantzopoulou, E. Kalogirou, A. Kalantzopoulos, H. Metaxa, R. Thede, N.A. Katsanos, V. Sotiropoulou, Chromatographia 46 (1997) 161.
[122] E. Van der Vlist, J. Van der Meijden, J. Chromatogr. 79 (1973) 1.
[123] R.G. Gerritse, J.F.K. Huber, J. Chromatogr. 71 (1972) 173.
[124] F. Roubani-Kalantzopoulou, V. Sotiropoulou, H. Metaxa, N.A. Katsanos, J. Microcol. Sep. 10 (1998) 141.
[125] V. Siokos, J. Kapolos, F. Roubani-Kalantzopoulou, Z. Phys. Chem. 216 (2002) 1311.
[126] Ch. Abatzoglou, N.A. Katsanos, A. Kalantzopoulos, F. Roubani-Kalantzopoulou, in: G.F. Froment, K.C. Waugh (Eds.), Reaction Kinetics and the Development of Catalytic Processes (Studies in Surface Science and Catalysis, vol. 122), Elsevier, Amsterdam, 1999.
[127] F. Roubani–Kalantzopoulou, I. Bassiotis, Th. Artemiadi, S. Margariti, E. Arvanitopoulou, N.A. Katsanos, Fresenius Environ. Bull. 10 (2001) 98.
[128] V.A. Bakaev, W.A. Steele, Langmuir 8 (1992) 1372.
[129] M.H. Abraham, C.F. Poole, S.K. Poole, J. Chromatogr. A 842 (1999) 79.
[130] G.A. Eiceman, H.H. Hill Jr., J. Gardea-Torresdey, Anal. Chem. 72 (2000) 137R.
[131] C.S. Poole, S.A. Schuette, Contemporary Practice of Chromatography, Elsevier, Amsterdam, 1984.
[132] E. Papirer, E. Brendle, J. Chim. Phys. Chim. Biol. 95 (1998) 122.
[133] E. Brendle, H. Balard, E. Papirer, J. Chim. Phys. Chim. Biol. 95 (1998) 1685.
[134] H. Balard, E. Papirer, A. Khalfi, H. Barthel, Compos. Interf. 6 (1999) 19.
[135] A. Kalantzopoulos, Ch. Abatzoglou, F. Roubani-Kalantzopoulou, Coll. Surf. A 151 (1999) 377.
[136] D. Gavril, A. Koliadima, G. Karaiskakis, Langmuir 15 (1999) 3798.
[137] N.L. Filippova, J. Coll. Interf. Sci. 197 (1998) 170.
[138] I. Kaya, Polym. Plast. Technol. Eng. 38 (1999) 385.
[139] C.F. Poole, The Essence of Chromatography, Elsevier, Amsterdam, 2003.
[140] M. Frere, M. Zinque, K. Berlier, R. Jadot, Adsorption 4 (1998) 239.
[141] M.J. Bojan, A.V. Vernov, W.A. Steele, Langmuir 8 (1992) 901.
[142] L. Matranga, A.L. Myers, E.D. Glandt, Chem. Eng. Sci. 47 (1992) 1569.
[143] R.F. Cracknell, P. Gordon, K.E. Gubbins, J. Phys. Chem. 97 (1993) 494.
[144] J. Jagiello, J.A. Schwarz, Langmuir 9 (1993) 2513.
[145] U. Huber, F. Stoeckli, J.P. Houriet, J. Coll. Interf. Sci. 67 (1978) 195.
[146] M.M. Dubinin, Carbon 23 (1985) 373.
[147] M. Jaroniec, J. Pietrowska, Monatsh. Chem. 117 (1986) 7.
[148] M.M. Dubinin, G.M. Planvik, Carbon 6 (1968) 183.
[149] P. Brauer, H.R. Poosch, M.V. Szombathely, H. Heuchel, M. Jaroniec, in: M. Suzuki (Ed.), Fundamentals of Adsorption, Elsevier, Amsterdam, Kodansha, Tokyo, 1993.
[150] M. Heuchel, P. Brauer, M.V. Szombathely, M. Jaroniec, in: J. Rouquerol, et al. (Eds.), Characterization of Porous Solids III, Elsevier, Amsterdam, 1994, p. 633.
[151] J. Jagello, T. Bandosz, K. Putyera, J.A. Schwartz, in: J. Rouquerol, et al. (Eds.), Characterization of Porous Solids III, Elsevier, Amsterdam, 1994, p. 679.
[152] S. Skrabakova, E. Matisova, M. Onderovo, I. Novak, D. Berek, Chem. Pap. 48 (1994) 169.
[153] E. Matisova, S. Skrabakova, J. Chromatogr. A 707 (1995) 145.
[154] A. Gierak, M. Seredych, in: W. Rudzinski (Ed.), Annales Universitatis Mariae Curie-Sklodowska, Lublin, 2002, p. 119.
[155] N.A. Katsanos, F. Roubani-Kalantzopoulou, in: W. Rudzinski (Ed.), Annales Universitatis Mariae Curie-Sklodowska, Lublin, 2002, p. 101.

[156] A.P. Terzyk, P. Kowalczyk, A. Gauden, in: W. Rudzinski (Ed.), Annales Universitatis Mariae Curie—Sklodowska, Lublin, 2002, p. 75.
[157] P. Kowalczyk, A. Gauden, A.P. Terzyk, D.D. Do, G. Rychlicki, in: W. Rudzinski (Ed.), Annales Universitatis Mariae Curie—Sklodowska, Lublin, 2002, p. 46.
[158] S. Faramawy, A.M. El-Fadly, A.Y. El-Naggar, A.M. Youssef, Surf. Coat. Technol. 90 (1997) 53.
[159] F. Rubio, J.L. Oteo, J. Mater. Sci. Lett. 11 (1992) 1501.
[160] F.L. Matthews, R.D. Rawlings, Composite Materials: Engineering and Science, Chapman and Hall, London, 1993.
[161] R.R. Tummala, Borate Glasses. Material Science Research, Plenum Press, New York, 1977.
[162] M. Pyda, B.S. Stanley, M. Xie, G. Guiochon, Langmuir 10 (1994) 1573.
[163] J. Jagiello, G. Ligner, E. Papirer, J. Coll. Interf. Sci. 137 (1990) 128.
[164] M. Jaroniec, in: A. Dabrowski, V.A. Tertykh (Eds.), Adsorption on New and Modified Inorganic Sorbents, Elsevier, Amsterdam, 1996.
[165] E. Papirer, H. Balard, in: A. Dabrowski, V.A. Tertykh (Eds.), Adsorption on New and Modified Inorganic Sorbents, Elsevier, Amsterdam, 1996.
[166] C. Erkey, G. Madras, M. Orejuela, A. Akgerman, Environ. Sci. Technol. 27 (1993) 1225.
[167] P. Foley, N. Gonzalez-Flesca, I. Zdanevitch, J. Corish, Environ. Sci. Technol. 35 (2001) 1671.
[168] C.-T. Hsich, J.-M. Chen, J. Coll. Interf. Sci. 255 (2002) 248.
[169] O. Inel, D. Topaloglu, A. Askin, F. Tumsek, Chem. Eng. J. 88 (2002) 255.
[170] C. Bertoncini, J. Raffaelli, L. Fassino, H.S. Odetti, E.J. Bottani, Carbon 41 (2003) 1101.
[171] P. Kluson, S.J. Scaife, J. Porous Mater. 9 (2002) 115.
[172] M.M.L. Ribeiro Carrott, A.J.E. Candeias, P.J.M. Carrott, P.I. Ravikovitch, A.V. Neimark, A.D. Sequeira, Microporous Mesoporous Mater. 47 (2001) 323.
[173] J. Castellano, N. Snow, J. Agric. Chem. 49 (2001) 4296.
[174] R.P. Baptista, A.M. Santos, A. Fedorov, J.M.G. Martinho, C. Pichot, A. Elaissari, J.M.S. Cabral, M.A. Taipa, J. Biotechnol. 102 (2003) 241.
[175] M. Kruk, M. Jaroniec, J. Choma, Carbon 36 (1998) 1447.
[176] W. Steele, Langmuir 15 (1999) 6083.
[177] E. Bottani, W. Steele, Adsorption 5 (1999) 81.
[178] L.P. Ding, S.K. Bhatia, Carbon 39 (2001) 2215.
[179] A. Kalantzopoulos, H. Zahariou-Rakanta, F. Roubani-Kalantzopoulou, Anal. Lab. 6 (1997) 149.
[180] F. Roubani-Kalantzopoulou, N.A. Katsanos, A. Kalantzopoulos, Chimica Chronica 26 (1997) 391.
[181] A.L. Dent, R.J. Kokes, J. Phys. Chem. 73 (1969) 3781.
[182] R.J. Kokes, A.L. Dent, Adv. Catal. 22 (1972) 1.